Recent synthetic transport systems

Matile, Stefan; Vargas Jentzsch, Rodrigo Andreas; Montenegro Garcia, Javier; Fin, Andréa

How to cite

MATILE, Stefan et al. Recent synthetic transport systems. In: Chemical Society reviews, 2011, vol. 40, n° 5, p. 2453–2474. doi: 10.1039/c0cs00209g

This publication URL: https://archive-ouverte.unige.ch/unige:15007
Publication DOI: 10.1039/c0cs00209g

Recent synthetic transport systems

Stefan Matile,*[a] Andreas Vargas Jentzsch,[a] Javier Montenegro[a] and Andrea Fin[a]

This critical review covers progress with synthetic transport systems, particularly ion channels and pores, between January 2006 and December 2009 in a comprehensive manner. This is the third part of a series launched in the year 2000, covering a rich collection of structural and functional motifs that should appeal to a broad audience of non-specialists, including to organic, biological, supramolecular and polymer chemists. Impressive breakthroughs have been achieved over the past four years in part because of a fruitful expansion toward new types of interactions, including metal-organic, π-π, aromatic electron donor-acceptor, anion-π or anion-macrodipole interactions as well as dynamic covalent bonds.

1 Introduction

This review comprehensively covers progress with synthetic transport systems published during the period from January 2006 to December 2009. It continues a series that was initiated with a summary of the period from January 2000 to December 2003 in *Tetrahedron*, followed by part two in this journal covering January 2004 to December 2005.[1,2] This series complements excellent reviews of the topic from other groups[3-5] as well as more focused accounts and highlights on specific topics.[6-14]

After briefly reiterating essential terms, definitions and methods in the introduction, we continue with the traditional, completely subjective prelude on new sources of inspiration, this time on the expansion of our repertoire of interactions available to create function. The main part of the review takes off with one of the highlights of this period, that is the introduction of metal-organic architectures.[6] The "heavy-metal" chapter 3.1 is followed by a summary of the similarly innovative emergence of π,π-architectures in chapter 3.2.[7] Functional innovation is covered in chapter 3.3 with the application of anion-π interactions to anion transport,[8] followed by a rich collection of small molecules in capable to do the same in many different ways.[9,10] Chapter 3.5 on steroid scaffolds is inserted to bridge between small anion transporters in chapter 3.4 and macrocycles in chapter 3.6. Innovative peptoid, arylamide or urea/amide macrocycles lead to peptide-based systems in chapter 3.7. The closing chapter 3.8 on synthetic polymers[13,14] is followed by a brief epilogue to wrap up and look forward.

Before launching the promised overview over the past four years of research, a brief recapitulation of basic terms and definitions seems appropriate. The experienced reader is encouraged to skip this part and move on to the main chapter, whereas the beginner might benefit from consulting also more detailed versions on concepts and techniques in preceding parts of the series.[1,2] More detailed descriptions are available as well.[15] The "synthetic transport systems" covered in this review are defined as molecules or groups of molecules that 1) feature significant structural motifs that do not occur in nature and 2) mediate transport in lipid bilayer membranes. Excluded by this definition are peptides and proteins with chemical or bioengineered modifications only, natural products, artificial membranes such as porous materials, and so on. Focus is on ion channels and pores. The term synthetic transport systems, however, is selected and defined as non-specific from a mechanistic point of view. In principle, it can cover ion carriers, ion channels, pores, detergents, flippases, endovesiculators, fusogens, and the like (Fig. 1). This non-binding terminology is preferred because transport mechanisms are sometimes intrinsically obscure, depend on conditions and are thus often not exclusive for a given system.

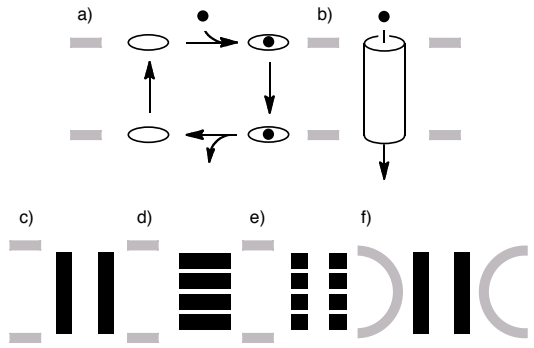

Fig. 1. Schematic transport mechanism of (a) ion carriers and (b) ion channels and schematic active structures of channels and pores covering (b) unimolecular, (c) barrel-stave, (d) barrel-hoop, (e) barrel-rosette and (f) micellar architectures.

Detergents (or surfactants) disassemble (or lyse) lipid bilayer membranes, usually producing mixed micelles. Pores, channels and carriers act in intact or only locally damaged lipid bilayers. With better alternatives still missing, channels and pores remain defined as compounds that feature single-molecule currents in planar bilayer conductance experiments. They are thought to mediate fast translocation without moving

[a]*Department of Organic Chemistry, University of Geneva, Geneva, Switzerland. Fax: +41 22 379 5123; Tel: +41 22 379 6523; E-mail: stefan.matile@unige.ch; www.unige.ch/sciences/chiorg/matile*

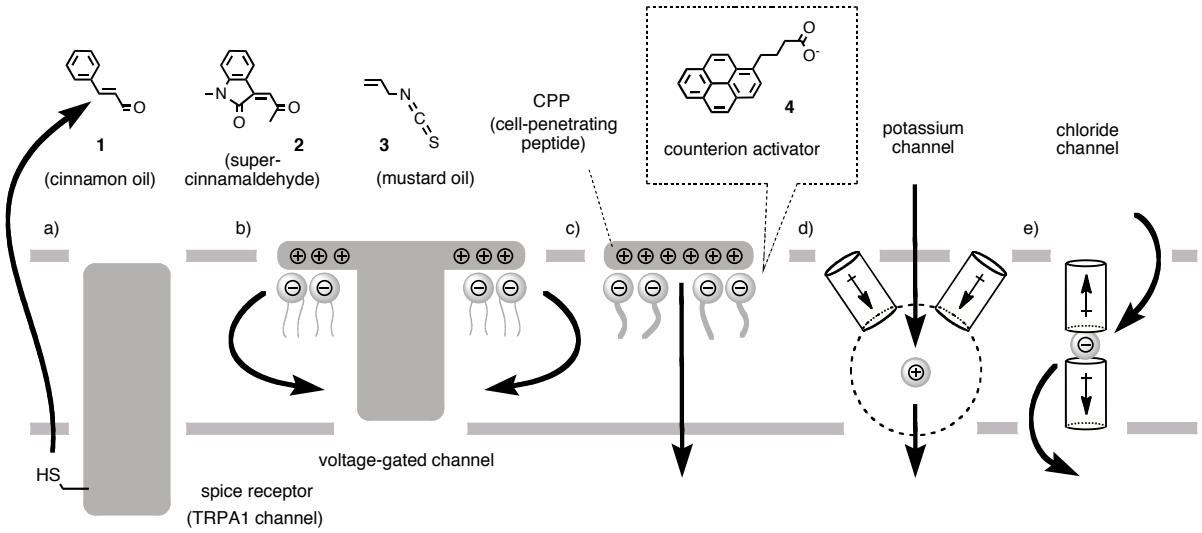

Fig. 2 "Exotic" interactions as new sources of inspiration: (a) Covalent capture chemistry with spice receptors leading to the super-spicy cinnamaldehyde **2**, polyion-counterion chemistry accounts for (b) the voltage-gating of potassium channels and (c) the cellular uptake of CPPs, and interactions with macrodipoles for the selectivity of potassium and chloride channels.

significantly by themselves (Fig. 1b). Carriers shuttle more slowly and together with the cargo across the membrane (Fig. 1a). They are too slow to generate detectable single-channel currents in planar bilayers. They can, however, also shuttle across macroscopic bulk liquid membranes, where "pure" ion channels are inactive. Carriers are thus best identified in the U-tube. However, it is important to highlight that the absence of single-channel currents and inactivity in the U-tube do not necessarily exclude the existence of ion channels/pores and ion carriers, respectively, that single-channel currents do not exclude activity in the U-tube, and so on.

Ion channels transport inorganic salts, whereas the larger pores transport molecules as well. On the structural level, channels and pores have been classified according to unimolecular (Fig. 1b), barrel-stave (Fig. 1c), barrel-hoop (Fig. 1d), barrel-rosette (Fig. 1e) or micellar architectures (Fig. 1f). In micellar pores, the bilayer membrane is locally micellized to become part of the active, usually short-lived suprastructure.[1,2] Important characteristics to look for with synthetic transport systems include ion selectivity, homogeneity on the single-molecule level, inertness of the active structure (long lifetimes), instability, and responsiveness toward voltage, pH, light as well as chemical stimulation (ligand gating, blockage).

2 New sources of inspiration

Traditional design strategies for supramolecular functional architectures in general employ a surprisingly limited repertoire, focusing mostly on five standard interactions, hydrogen bonding, hydrophobic interactions, ion pairing, π,π-interactions and cation-π interactions. Efforts to expand this "chemical code" for the creation of supramolecular systems are of fundamental importance well beyond the scope of this review. The most significant progress in the field over the past four years concerns the consideration of metal-organic architectures, covalent capture, π-π architectures, anion-macrodipole and anion-π interactions. Some sources of inspirations behind these past and possible future breakthroughs on the expansion of the "chemical code" with synthetic transport systems are briefly spotlighted in the following, moving from covalent capture chemistry, polyion-counterion and anion-macrodipole interactions to the more adventurous anion-π interactions and anion-halogen bonding interactions (Figs. 2 and 3).

Covalent capture chemistry received much attention in recent results concerning the molecular basis of the sensation of spiciness.[16] Responsible for this flavor-independent phenomenon of burning pain is TRPA1, an ion channel composed of six transmembrane helices. To make the hot feeling really last, the weak interactions accounting for common molecular recognition processes are complemented by more serious dynamic covalent capture chemistry. Cinnamaldehyde **1**, the spicy component of cinnamon oil, for example, suffers a conjugate addition from thiol nucleophiles of specific cysteine residues in the large cytoplasmatic domain which activates the TRPA1 channel covalently (Fig. 2a). To demonstrate the validity of this hypothesis, the supercinnamaldehyde **2** with an enhanced Michael acceptor was designed, synthesized and shown to exert infernal spiciness. The same covalent capture mechanism applies to mustard oil, where the allyl isothiocyanate **3** is attacked to yield the dithiocarbamate and open the TRPA1 channel.

Polyion-counterion interactions are finally beginning to receive appropriate recognition in biological transport systems.[17-19] Polyion-counterion interactions originate from proximity effects to minimize intramolecular charge repulsion and are fundamentally different, similarly labile yet much stronger than simple ion pairs.[19] Polyion-counterion interactions have been found to account for two of the most controversial biological transport processes. Firstly, the puzzling entry of cell-penetrating peptides (CPPs) into cells by passive diffusion across the plasma membrane has now been understood as multiple counterion hopping process (Fig. 2c). For CPPs to enter the membrane, their hydrophilic counterions are exchanged by amphiphilic ones. The reverse

process takes place for CPPs to leave the membrane on the cytosolic side to ultimately end up bound to an internal polyanion such as RNA.[17] Based on this mechanistic insight, amphiphilic counterions such as pyrenebutyrate **4** have been found to act like translocation catalysts and enable direct cytosolic delivery by kinetically outcompeting alternative endocytosis pathways.

The second polyion-counterion process of current interest concerns the voltage gating of potassium channels. To open these channels, cationic, arginine-rich domains move across the membrane in response to membrane polarization. This process is now understood as mediated by anionic phospholipids counterions, and polyion-counterion interactions are identified as new possible target for drugs and neurotoxins (Fig. 2b).[18] As with cellular uptake of CPP, the central role of polyion-counterion interactions for voltage gating has been predicted with synthetic transport systems[19] and is known to apply as charge-inverted system for gene transfection.[20] The slow identification and reluctant acceptance of polyion-counterion interactions at work may originate from their dynamic nature, incompatible with covalent structure determination by X-ray crystallography.

Cellular retinal-binding protein (CRALBP), a protein in charge of transmembrane transport of used *all-trans* retinal for regeneration, contributes one (out of many) corroborative example for the importance of polyion-counterion interactions.[21] CRALBP translocation is triggered by the binding of anionic lipid counterions to arginine clusters, mutation of single arginines compromises regeneration and is associated with Bothnia dystrophy.

The same potassium channels are admired since some time as most beautiful example for the power of macrodipole-cation interactions.[22] Here, a potassium ion is "bound" in free space, in bulk water, without direct physical contact, at the focal point of the negative end of the macrodipoles of four α-helices. Similarly spectacular use of macordipoles has since been found to regulate chloride channels,[22] and phosphate recognition in biology occurs quite reproducibly at the positive end of α-helical dipoles.[23] Arguably the most inspiring recent contribution to the topic comes from catalysis, where the reactive enolate intermediate **5** of the Julia-Colonna epoxidation is enantioselectively stabilized at the N-terminus the α-helical catalyst by a combination of short-range hydrogen bonding and long-range macrodipole-anion recognition (Fig. 3).[24-26] This example illustrates how lessons learned on anion recognition by "exotic interactions" on the ground state could be directly applicable to transition-state stabilization, i.e., catalysis.

Contrary to the preceding examples, anion-π interactions and anion-halogen interactions are much less accepted, in part still controversial in theory or even largely unknown. Anion-π interactions received much theoretical interest over the last decade, with experimentally support coming mainly from solid state.[27-33] This is understandable. Contrary to the cation-π interactions on usual, π-basic aromatics with negative quadrupole moments, anion-π interactions require access to the unusual, π-acidic aromatics with inverted, positive quadrupole moments. The few available studies on anion-π interactions in solution seek assistance from additional contributions such as hydrogen bonding or ion pairing and are thus not always conclusive. A recent leading example is the nitrophenyl quartet **6**, where an underlying calix[4]pyrrole receptor is placed to enhance eventual anion-π interactions (Fig. 3).[33] Although only weakly π-acidic, nitrophenyl quartets are found to still contribute to anion binding with 0.4 kJ/mol. Decreasing π-acidity in phenyl quartets reduces affinity, more π-acidic quartets were not reported. During the period of this review these weak anion-π interactions have been proposed as useful in synthetic transport systems.[8] This implication suggests that synthetic transport systems could be applied as a tool to explore the functional relevance of other weak interactions. New interactions identified by synthetic transport systems could be of interest in catalysis, where similarly weak interactions work best (see below).

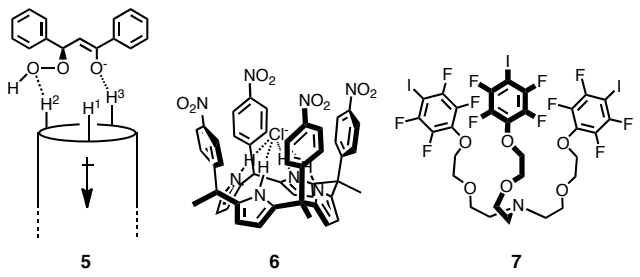

Fig. 3. "Exotic" interactions as new sources of inspiration: Interactions with macrodipoles possibly contribute to the stabilization of the reactive intermediate **5** in the Julia-Colonna epoxidation, anion-π interactions are explored in receptor **6**, anion binding with halogen bonds in receptor **7.**

The concept of synthetic transport systems as probes for weak interactions at work could be fruitful to, for example, elaborate on the possible functional relevance of anion-halogen interactions. Halogen bonds are increasingly recognized as complements to hydrogen bonds,[34] biological relevance from thyroxine and related thyroidal hormones is attracting increasing interest for medicinal applications,[35] and numerous breakthroughs in crystal engineering have been reported.[36] The obvious implications on anion binding have been explored so far in a single pioneering example, where eventual anion binding to up to three iodine donors is enhanced by cation binding to the proximal binding site in the tripodal receptor **7**.[37]

3 Synthetic transport systems 2006-2009

After introduction and a few new and totally subjective sources of inspiration, here comes the central part of this review. The comprehensive summary of synthetic transport systems created between January 2006 and December 2009 beginning with metal-organic architectures, π-π architectures and anion-π interactions as highlights of this period. General trends include an impressive expansion of structural diversity, particularly with regard to small anion transporters, macrocyles and polyion-counterion systems besides a steady progress with the classics such as steroids, calixarenes, cyclodextrins, crown ethers, peptide mimics and synthetic polymers.

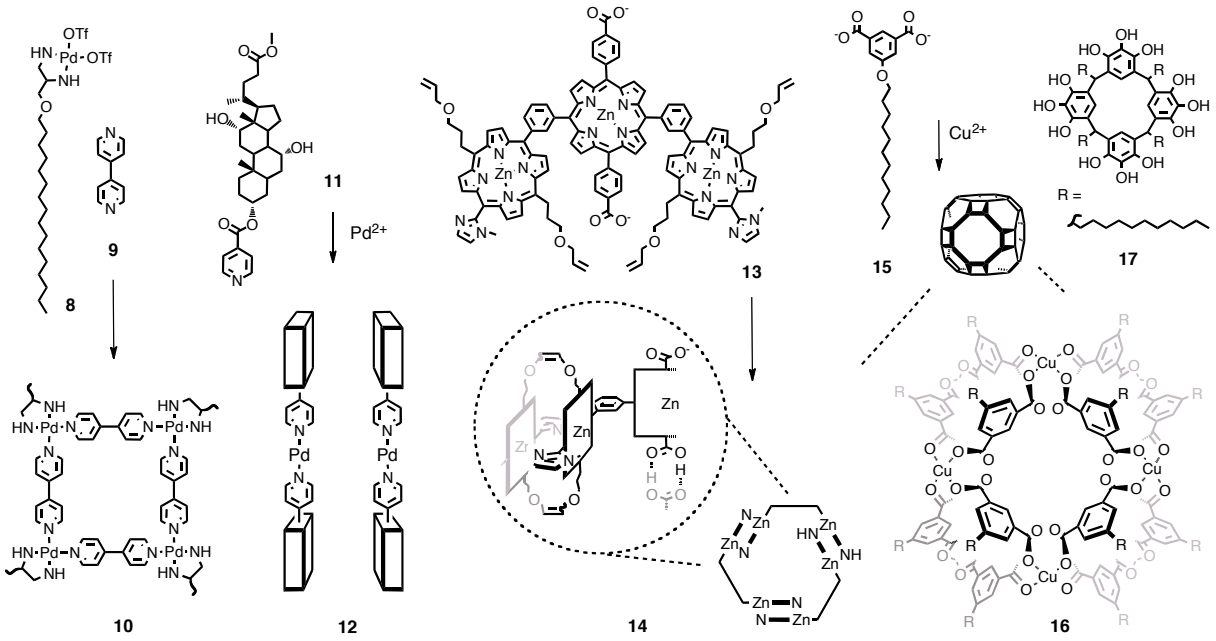

Fig. 4. Recent synthetic transport systems with metal-organic scaffolds: An amphiphilic coordination square **10**, Pd-gated cholate bundle **12**, covalently captured porphyrin metallopores **14**, MOPs **16** and Cu-capsules from gallarane **17**.

3.1 Metal-organic architectures

Metal-organic scaffolds entered the field during the period covered by this review.[6] A revolutionary design from the Fyles group came first.[38] The assembly of Pd-amphiphiles **8** and bipyridine **9** was expected to produce the hollow shape-persistent coordination squares **10** with hydrophobic tails to insert into the membrane (Fig. 4). Channels consistent with internal diameter, short lifetime and rare occurrence expected for the complex metal organic architecture **10** were observable in single-channel recordings among other active systems of unknown origin.

Another very innovative concept was developed to create the first "heavy-metal" channels that open in response to chemical stimulation.[39] As facial amphiphiles, cholates such as **11** self-assemble into single-leaflet bundles. Addition of Pd^{2+} then crosslinks two bundles by coordination to the pyridines in the middle of the membrane and produces the active transmembrane "barrel-rosette" architectures **12** (Figs. 4 and 1e). An elegant series of ion transport experiments in vesicles with an internal fluorescent probe was used to demonstrate that addition of Pd^{2+} from both sides of the bilayer produces active channels, whereas Pd^{2+} removal with hexathia-18-crown-6 causes inactivation. The design of ligand-gated synthetic transport systems is one of difficult and least studied topics in the field.[1,2] The realized application of metal-organic scaffolds for this purpose therefore is a very important breakthrough not only from a structural but also from a functional point of view.

The third breakthrough approach toward metal-organic synthetic transport systems uses the self-assembly of oligoporphyrin **13**.[40] Aromatic turns inserted between the three zinc porphyrins and imidazole ligands at both ends assure that axial coordination of imidazole ligands to the zinc produces a trimeric pore. These macrocycles are then stabilized by covalent capture using Grubbs ring-closing metathesis. Dimerization of the resulting single leaflet pores, possibly assisted by top hydrogen bonding between carboxylic acids, gives the expected active "barrel-hoop" architecture **14**. In planar bilayer conductance experiments, metallopore **14** is long-lived, ohmic and homogenous. The nS-conductance level is as large as expected for the important inner diameter. Cation selectivity, permeability of cations as big as tetrabutylammoniums and reversible blockage by fourth generation PAMAM dendrimers are consistent with the functional role of carboxylates at the pore entrance. This brilliant study further represents the first example for the application of covalent capture to synthetic transport systems described in this review.

The fourth key approach toward metal-organic synthetic transport system concerns the assembly of isophthalate amphiphile **15** and $CuOAc_2$ into the metal-organic polyhedron (MOP) **16**.[41] Small, ohmic, long-lived, homogenous, cation selective single-channel conductance levels were consistent with cation flux through the channels in cuboctahedron **16**. A weak Eisenman XI selectivity and blockage by the permeant cation indicated strong cation binding.

The similarity of the channels in MOP **16** with the interior of calixarenes implied possible contributions of cation-π interactions to cation selectivity. This similarity was further underscored by the copper-mediated assembly of gallarene **17** into metallocapsules similar to MOP **16**.[42] The obtained single-channel conductance levels were small, ohmic, homogenous and cation selective. The gallarene amphiphiles **17** were later on found to form ion channels in the absence of copper as well, similar to other amphiphilic calixarenes (see chapter 3.6).[43]

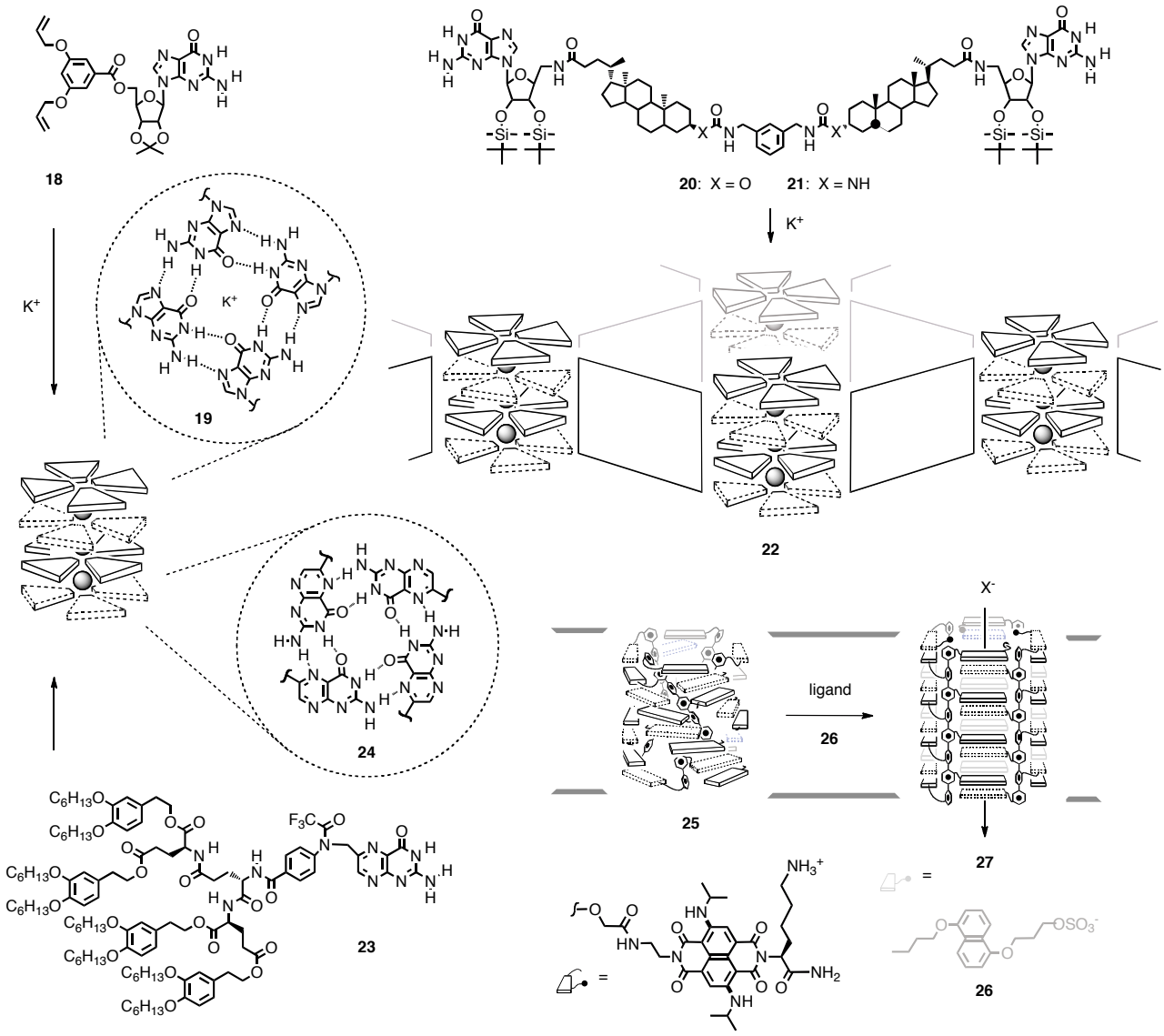

Fig. 5. Recent design strategies for synthetic transport systems with π-π architectures: Covalently captured G-quartets **19**, G-quartet scaffolds for cholate pores **22**, dendritic folate quartets **24** and π-stacked photosystems **25** that untwist in response to intercalators **26** into barrel-stave ion channels **27**.

3.2 π-π Architectures

Ubiquitous in chemistry, with examples reaching from DNA in biology to semiconductors in materials sciences, π-π architectures entered the field of synthetic transport systems around the beginning to the covered period.[7] This reluctant application of an established motif is understandable considering that at least the external domains of synthetic transport systems exist in a hydrophobic environment where dispersion components of π-π interactions are weak.

The first example builds on the assembly of guanosines such as **18** into G-quartets, which in turn π-stack on top of each other to produce barrel-rosette architectures **19** with a string of potassium cations bound in the middle (Fig. 5).[44] However, when simply added to lipid bilayers, the hydrophobic guanosine **18** was inactive in all assays. Active transport systems were obtained by covalent capture of G-quartet architectures **19** by ring-closing olefin metathesis (RCM). The increased stability of unimolecular G-quartet architectures **19** upon covalent capture was further supported by the π-stacked G-quartet signature in the CD spectrum measured in lipid bilayers. This is the second occurrence in this period where covalent capture has been essential to generate synthetic transport system.[40,44]

Permanent nucleoside dimerization with lithocholate spacers in **20** and **21** produced not only small ion channels expected for isolate G-quartet π-stacks with cross-linked nucleosides (<0.1 nS conductance) but also large pores.[45,46] These results suggested that G-quartet π-stacks can also serve as "metal-organic" scaffolds that are then connected with lithocholate spacers to produce the active "metal-organic framework" (MOF) pores **22**. The giant metallopores **22** were cation-selective (P_{K^+}/P_{Cl^-} = 6.4) and had very large conductance levels (1-5 and >20 nS). Increased single-molecule lifetimes in response to the replacement of the carbamates in **20** by ureas in **21** supported the importance of hydrogen-bonded chains to stabilize the metallopores **22**.[46]

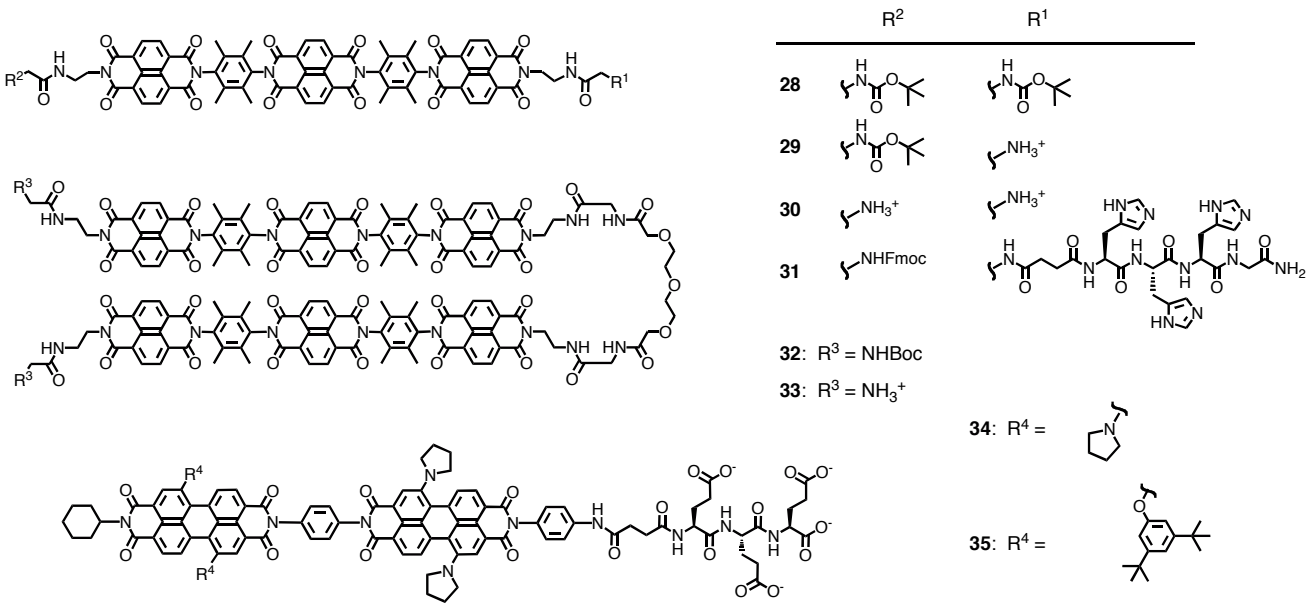

Fig. 6. Recent synthetic transport systems that operate with anion-π interactions.

Complementary and in parallel to the use of hydrophobic G-quartets as ion channels and pores, hydrophilic G-quartets trapped within vesicles have been introduced to detect activity and selectivity of ion channels by circular dichroism spectroscopy.[47]

Whereas the stability of hydrophobic G-quartets **19** in membranes was insufficient without covalent capture to form functional ion channels, folate dendrimers **23** were capable to self-assemble into functional ion channels **24** without extra stabilization by covalent capture.[48] Exergonic self-assembly with saturation behavior in the Hill plot produced the CD signature of stacked folate quartets **24**. The activity of folate quartet channels **24** was characterized by the absence of non-specific leaks, cation selectivity (P_K+/P_{Cl}- = 4.9, Eisenmann I sequence) and low single-channel conductance (19 (69%), 14 (27%), 7 (14%) pS), homogenous and ohmic, roughly as expected for folate quartets **24** (d_{Hille} = 3.7 Å). The ionophoric properties of folate quartets **24** were correctly reflected in blockage by the permeant cation (EC_{50} (K^+) = 230 mM, g_{MAX} = 21 pS).

The construction of helical, π-acidic π-stack architectures such as **25** has been achieved for colorless systems before the period covered in this review.[2] The intercalation of π-basic ligands **26** increases the π-stack repeat and untwists the closed helix into open, ligand-gated barrel-stave ion channels such as **27**. During the current period, the π-stack architecture **25** was colored in blue using NDI fluorophores with alkylamino donors in the core.[49] Transient absorption spectroscopy with π-stack **25** showed that the introduction of this new, compact (i.e., atom-efficient) chlorophyll mimic provided access to ultrafast (<2 ps) photoinduced charge separation. This process occurred quantitatively (>97%) and lasted relatively long (61 ps, >400 ns in vesicles). In vesicles with external electron donors and internal quinone acceptors, π-stack **25** exhibited photosynthetic activity and produced a pH gradient with light. The Hill coefficient n = 4 confirmed the supramolecular nature of the photosystems as well as endergonic self-assembly. Intercalation of ligand **26** transformed the photosystem **25** into the ligand-gated ion channel **27**.

3.3 Anion-π interactions

Whereas cation-π interactions have been used before to build synthetic transport systems, anion-π transporters have appeared first during the current period (Fig. 6).[8] As outlined in the chapter on new sources on inspiration, this is quite remarkable because little is known about anion-π interactions beyond theoretical studies and crystal engineering, not to speak of using anion-π interactions to create functional architectures.[27-33]

To explore the usefulness of anion-π interactions to transport anions across lipid bilayers, a small collection of oligo-*p*-phenyl-*N*,*N*-naphthalenediimides (O-NDIs) **28**-**33** and -perylenediimides (O-PDIs) **33**-**34** has been made and studied (Fig. 6). Computational studies were in agreement with the occurrence of anion-π interactions. The quadrupole moments Q_{zz} ~ +19 B found for NDIs are twice as large as with hexafluorobenzene and in the range of TNT.[50,51] Routine assays in fluorogenic vesicles suggested that O-NDI rods **29** with one charged ammonium terminus have higher activity.[50] The activity of uncharged O-NDI rods **28** was weaker, that of O-NDI rods **30** with charges at both termini the weakest. The same trends were found with dimeric O-NDI rods, where the uncharged **32** was clearly more active than dication **33**.[51] Increasing hydrophilicity and charge at one rod terminus from a single ammonium in **29** to a short cationic peptide in **31** resulted in a dramatic increase in activity.[52]

All active O-NDI rods **28**-**33** preferred to transport anions rather than cations across lipid bilayer membranes. The most active cationic O-NDIs **29** exhibited a rather weak halide IV selectivity sequence (Cl^- > Br^- > I^- > F^-). The less active,

neutral O-NDIs **28** showed a more pronounced halide VI topology ($Cl^- > F^- > Br^- > I^-$), covalent capture as O-NDI hairpins **32** further enhanced chloride selectivity. These trends from end-group engineering and covalent capture suggested that self-assembly into transmembrane O-NDI bundles is essential, with activity decreasing and selectivity increasing with increasingly close contacts. Trends toward anti-Hofmeister topologies implied that anion affinities are strong enough to overcompensate eventual costs of dehydration, similar selectivity for F^- and OAc^- that selectivity originates from energetics rather than size exclusion. A significant anomalous mole fraction effect (AMFE), that is underadditive activity of mixtures of "slow" and "fast" anions, could support multiion hopping along the π-acidic shape-persistent O-NDI scaffolds as transport mechanism, although other interpretations of this phenomenon cannot be excluded.

This experimental support for the functional relevance of anion-π interactions calls for fundamental backup as well as applications toward catalysis and optoelectronic materials. Usefulness in artificial photosynthesis has been elaborated with O-PDIs **34** and **35**.[53] O-PDIs **34** contains a green, π-acidic scaffold that is long enough to span a lipid bilayer. One anionic peptide terminus was added to assure delivery and transmembrane orientation. In fluorogenic vesicles, the π-acidic O-PDI rods **34** and **35** were about as anion selective as O-NDI rods **28-33**. In chromogenic vesicles with external electron donors and internal electron acceptors, O-PDI rods **34** exhibited photosynthetic activity. A Hill coefficient $n = 9$ demonstrated that a transmembrane bundle of at least nine O-PDIs is needed for activity, and that the active suprastructure is a minority component in the system (as sometimes in real life, when only a few do the work, while many stand around and watch).

The combination with selective anion transport is attractive to address one of the key limitations with artificial photosynthesis in lipid bilayers. Namely, directional transmembrane charge separation with light can polarize the membrane and cause saturation of the system after few turnovers only. The compensation of active electron transport in one direction with passive anion antiport offers an attractive approach to convert electrogenic into electroneutral photosystems. Insensitivity toward the presence of the proton carrier FCCP suggested that this is achieved with the anion-π photosystem **34**.

In photosystem **35**, the green diamino PDI in the inner leaflet of photosystem **34** are replaced by a red diaryloxy PDI. Positioning of the red PDI in the inner and the green PDI in the outer leaflet of the membrane is assured by the anionic terminus next to the green PDI. Compared to the unicolor photosystem **34**, the red PDI in dyad **35** are expected to help collecting more light and to mediate electron transfer from the green PDI down a redox gradient to the intravesicular acceptor. Increased photosynthetic activity was observed.

3.4 Small anion transporters

Anion transport is the field that has received most attention during the past years. Several excellent reviews have appeared.[4,5,9,10] The topic covers diverse structural motifs, and innovative interactions beyond ion pairing and hydrogen bonding are also explored. Anion transport with anion-π interactions has been the topic of the preceding chapter 3.3, anion transport with anion-macrodipole interactions will be summarized in the context of peptide mimics, and anion transport by macrocycles, peptide mimics, polymers or polyion-counterion complexes will be discussed in the respective chapters. Anion transport with small molecules deserves a separate chapter because research on this family has been particularly intense. However, given the rich secondary literature available, the description will be kept shorter than usual.

Prodigiosin, a red secondary metabolite from bacteria, has inspired the synthesis of the derivatives **36-43** (Fig. 7).[54] The more substantial tails, containing also ketones or esters, reduced chloride transport activity, whereas small ethyl tails as in **37** had little influence. Substitution of pyrroles in prodigiosin with methylimidazole-acetamido groups, isophthalamides or 2,6-dicarboxamido pyridines gave active HCl transporters **44-47**.[55] In an elegant study, isophthalamides **48-50** were prepared to confirm the importance of intramolecular hydrogen bonding in **49** to preorganize anion binding to the two amide hydrogen-bond donors and its consequences for transport across the membranes.[56] Decreasing activity of **49** with increasing pH was considered as additional support of the importance of preorganizing hydrogen bonds for activity, although other explanations certainly are conceivable. An inspired ^{13}C NMR assay was recently introduced to show that isophthalamides **50-52** facilitate transmembrane bicarbonate/chloride antiport.[57]

Isophthalate **53** with two amidoxy sidechains was found to form chloride channels in planar bilayers and in living cells. Amidoxy groups are interesting because their NH hydrogens are more acidic than amide hydrogens. Their acidity can be further enhanced by intramolecular H-bonding into so-called α-aminoxy turns (Fig. 7). The channel features high $Cl^- >> Br^-, I^-, NO_3^-$ selectivity and two dominant single-channel conductances at 54 and 108 pS.[58] The Hill coefficient $n > 1$ demonstrated the presence of an unstable, supramolecular active structure, the gating charge $z_g > 1$ non-ohmic behavior.[59] Amidoxyisophthalate **53** is one of the few synthetic ion channels that has been studied in living systems. Modulation of membrane potentials and of the coupled activity of voltage-gated calcium channels, intracellular calcium levels and the contraction of smooth muscle cells was observed.[59]

Anion transport activity was determined for amphiphilic biscatechols **54-59**.[60] Amphiphile **55** was best. Both longer and shorter alkyl chains reduced activity due to reduced partitioning into the membrane. Catechol methylation in **58** and catechol rearrangement in **59** removed all activity. Binding to the catechol hydrogen-bond donors rather than ion pairing with the protonated amine was proposed to determine activity and selectivity. A Hofmeister selectivity topology implied weak anion binding.

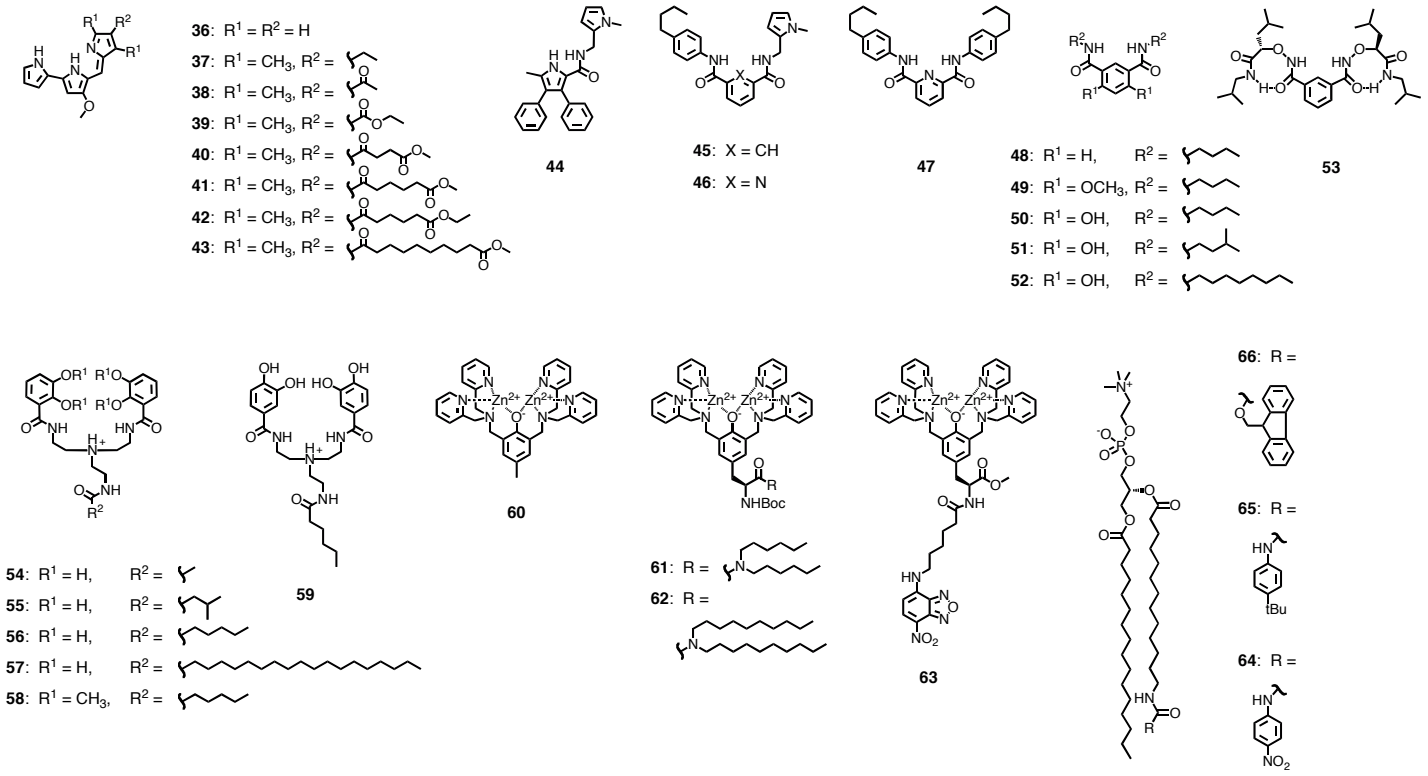

Fig. 7. Recent anion transport with small molecules includes preorganized hydrogen-bonding to isophthalates, best with α-aminoxy turns in **53**, catechols, or "dancing" ureas in lipid tails.

Dinuclear zinc complexes **60-63** were designed to transport anionic molecules including phospholipids across neutral and anionic lipid bilayers.[61,62] The more hydrophilic complex **60** was selective for anionic membranes and depolarized the cell membranes of Gram-positive bacteria. The labeled complex **63** could be used as fluorescent probe to image bacterial infection and tumors in animals.

The functionalized phospholipids **64-66** with hydrogen-bond donors at the end of one tail were conceived to transport anions across bilayer membranes with a new mechanism.[63] Extensive conformational changes were thought to make the functionalized tail "dance" up and down from membrane-water to leaflet-leaflet interface to grab and hand over the anions. Phospholipid **64** with terminal *para*-nitrophenyl ureas as strongest hydrogen-bond donors emerged as the most active chloride transporter. Inactivity with one-sided addition and increasing Hill coefficients with increasing membrane thickness were identified as convincing support for the proposed "dancing" mechanism.

3.5 Steroids

Steroid-based anion transporters such as **67-82**, also referred to as cholapods, are a classic in the field (Fig. 8).[64] In this approach, facially amphiphilic cholate scaffolds are equipped with carefully crafted anion binding sites. Extensive structure-activity relationships reported during the period of this review culminated in remarkably chloride selective transport in vesicles.[65] Transport activity was overall determined by the strength of the hydrogen-bond donors offered in the preorganized binding site. For instance, activation of ureas by *para*-nitrophenyl substituents improved activity, as did additional donors in position 3 of the steroidal A ring. However, several other factors contribute to an overall more complex phenotype. Increased hydrophobicity as in **70** had little importance. Interestingly, positive charges as in **82** removed anion transport activity, possibly, the authors argued, because too strong binding inhibited anion release.

Cationic cholates such as **83-87**, also referred to as ceragenins or CSAs, cationic steroid antibiotics, have been explored for decades.[66] During the period of this review, the ability of cholates **83-87** to mediate the efflux of anionic fluorophores or cationic quenchers from vesicles of different lipid composition has been explored.[67] Activity decreased with **84** > **83** > **85** > **86** > **87** and was best in vesicles composed of DOPE with 20% DOPG, followed by DOPG or DPPG with 50% cardiolipin, where the lysine-appended cholate **87** was particularly active. Activity in PE-rich vesicles was reflected in antibacterial activity. The antimicrobial activity correlated better with the content of PE in the bacterial membrane than whether or not the bacteria have an outer membrane.

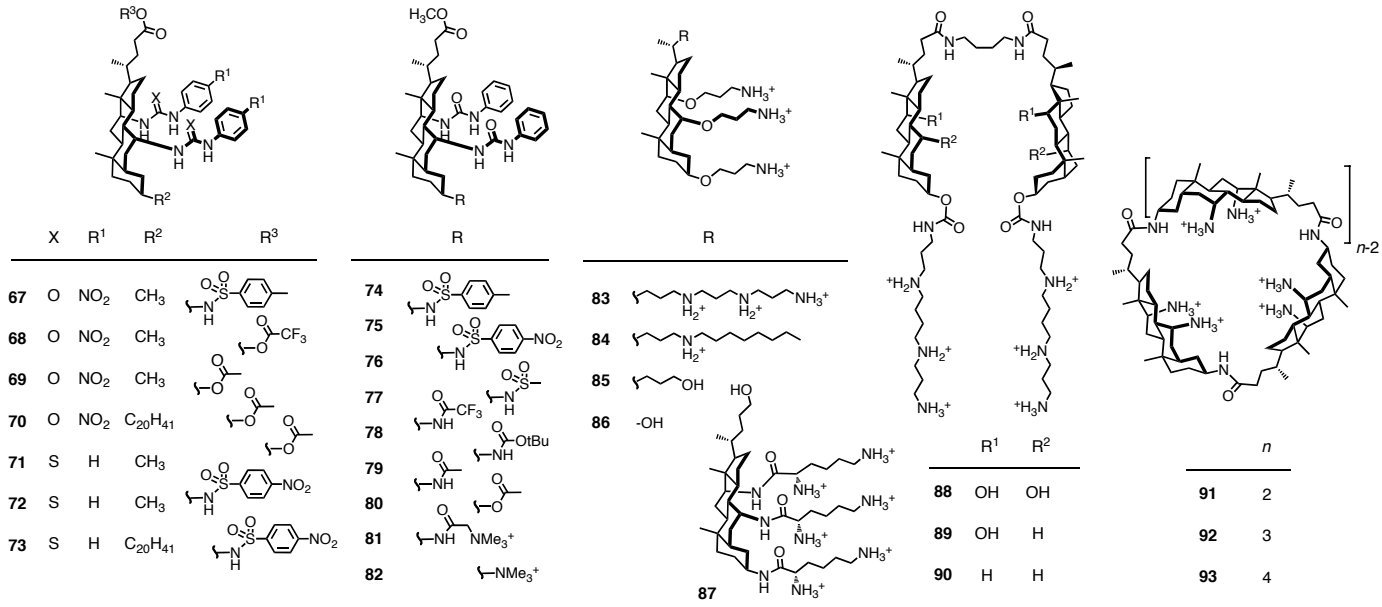

Fig. 8. Recent cholate transporters for anion transport include neutral and cationic monomers, dimers and cyclic oligomers. For dendritic oligomers, please see Fig. 9.

The ability of the dimeric cationic cholates **88-90** to accelerate the discharge of a transmembrane pH gradient increased with **90** < **89** < **88**, that is with increasing facial amphiphilicity of the cholate scaffold.[68] The Hill coefficient $n \sim 2$ indicated that the active structure is an unstable dimer. The antimicrobial activities correlated with the activities in anionic POPG vesicles but were inferior compared to monocholate controls.

Cationic cyclocholamides **91-93** have a lipophilic exterior and a cationic interior to include and transport anions by ion pairing (Fig. 8).[69] In vesicles, oligocholate macrocycles **91-93** were capable to transport chloride anions but not potassium cations, acting presumably as monomeric carriers.

Oligocholates **94-104** are readily synthesized from cholate, lysine and spermine or related polyamines (Fig. 9).[70-74] Because of their amphomorphic nature, these synthetic transport systems are also referred to as molecular umbrellas.[70] Whereas polyion-counterion systems achieve solubility in both hydrophilic and lipophilic environments by dynamic counterion exchange,[17-19] umbrellas **94-104** achieve this important adaptability to changing environments on the molecular level by means of rationally designed of amphomorphism. The facial amphiphilicity of the cholate scaffold is central to this research. To dissolve in hydrophilic environments, umbrellas **94-104** place the hydrophilic cholate faces on the surface and hide their hydrophobic faces in the interior. To dive into lipophilic environments such as a lipid bilayer, the hydrophobic cholate faces rotate to the surface of the umbrella and the hydrophilic faces hide in the interior. For release into hydrophilic environments, the hydrophilic cholate faces rotate back to the surface of the umbrella and the hydrophobic faces disappear in the interior. Covalent amphomorphism is a very important topic for traffic in general and cellular uptake in particular.

In umbrellas **94-98**, a hydrophilic fluorophore was attached initially to determine their position in bilayer membranes.[71] Depth quenching experiments revealed that sulfonated umbrellas **95** and **97** accumulate deeper in the membrane than their hydroxylated analogs **96** and **98**. This finding confirmed that the magnitude of amphomorphism, i.e. the facial amphiphilicity, determines the penetration depth into bilayer membranes. As a result, umbrellas with higher total charge enter better into hydrophobic environments.

Umbrella uptake into 95:5 POPC/POPG vesicles was found to accelerate with increasing size of the umbrella.[72] As expected for dominant amphomorphism, size-dependent uptake of more hydrophilic umbrellas **98** > **97** > **95** was better than that of less hydrophilic umbrellas **96** > **94**.

The subtle balance between transport and uptake known from polyion-counterion systems[1,2,17-19] was explored with umbrellas **99-101**.[73] The sulfonated umbrella **101** was active in pH discharge and Na^+ and Cl^- transport experiments, whereas the slightly more hydrophilic analogues **100** and **99** were not. However, under similar conditions, both umbrellas could cross bilayer membranes and enter into intact vesicles.

The neutral oligocholate homologs **102-104** were explored as thermally gated pores.[74] The high concentration, octamer **103** and dodecamer **104** mediated rapid sucrose release from 95:5 DPPC/DPPG vesicles under all explored conditions. Tetramer **102**, however, was active at 43 ºC but not at 37 ºC. At lower concentrations, octamer **103** and dodecamer **104** exhibited similar thermal gating. This phenomenon was thought to presumably originate from the known difference in partitioning of synthetic transporters into solid and fluid phase of DPPC bilayers.

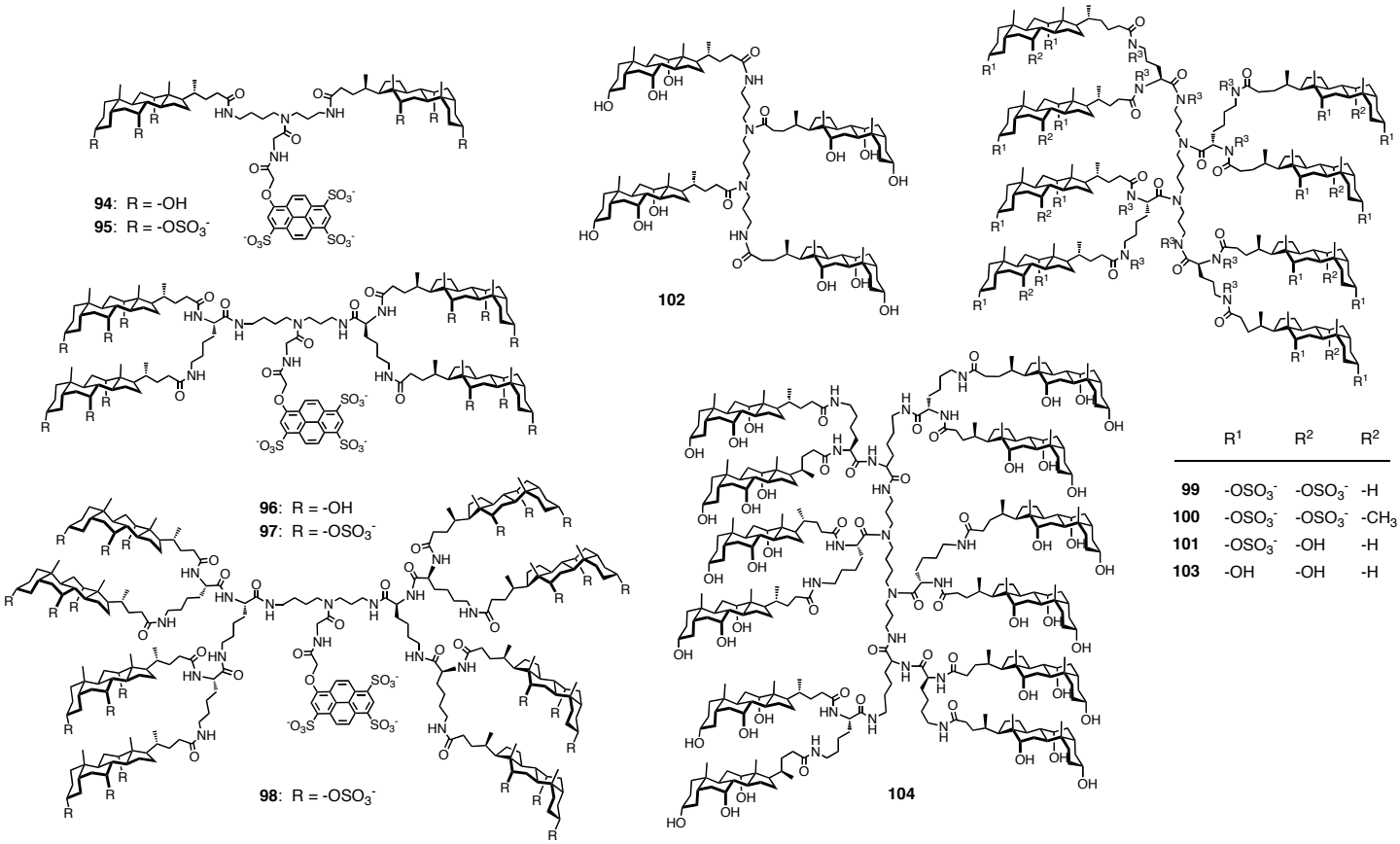

Fig. 9. Cholate oligomers as synthetic transport systems.

3.6 Macrocyclic transporters

The steroid motif as in cyclocholamides **91-93** is just one out of many explored in the context of macrocyclic transporters (Fig. 8). Innovative motifs from the covered period include calix[4]pyrroles **105-106** or cyclic oligoglycophosphodiesters **107-109** (Fig. 10). Calix[4]pyrroles can bind anions in the central focal point of their four NH-hydrogen bond donors (compare also Fig. 3). The *meso*-octamethyl calix[4]pyrrole **105** was found to mediate cesium-dependent chloride transport in POPC vesicles.[75] Transport was independent of the nature of the external anions but dependent on internal cations (Na^+, K^+, Rb^+ salts were not transported). The strapped calix[4]pyrrole **106** with an axial triazole CH-bond donor for strengthened anion binding, transported ion pairs independent of the nature of the countercation, possible due to the onset of complementary anion antiport (chloride/nitrate exchange).[76]

In cyclic oligosaccharides **107-109**, also referred to CyPLOS (cyclic phosphate-linked oligosaccharides), are anionic phosphodiester macrocycles that are decorated with long chains of different lipophilicity.[77] Interestingly, the most hydrophilic macrocycle was most active, the alkylated **109** was inactive. Ion transport in fluorogenic vesicles was independent of the nature of the cation and showed a weak Hofmeister selectivity ($I^- > Br^- > Cl^- > F^-$, halide I). More hydrophilic anions are not transported (glutamate, sulfate, F^-). Anion selectivity by anionic oligoether transporters **107-109** is certainly intriguing and deserves further investigation.

The cyclodextrin motif was present in the first synthetic ion channel, published by the Tabushi group in 1982.[78] In the Tabushi original, the hydrophobic tails were long enough to span a single leaflet of a lipid bilayer and thus implied the formation of a dimeric active structure of the formal barrel-hoop type. The less hydrophobic tails in cyclodextrins **110-112**, however, are long enough to span a full bilayer. They should thus formally act as unimolecular ion channel. The pH dependence of the activity of cyclodextrin channels **110** was determined with Na NMR and fluorescence assays with the chloride selective probe lucigenin entrapped within vesicles.[79] With decreasing pH, the amine groups at the lower rim of the macrocycle are increasingly protonated. Increasing charge repulsion as well as ion pairing was mentioned to explain the observed decreasing ion transport rate with decreasing pH. At high pH, both anion and cations were transported. Hofmeister selectivity for anion transport at lower pH implied that anion binding by the cationic channel is weak and cannot overcompensate the cost of dehydration.

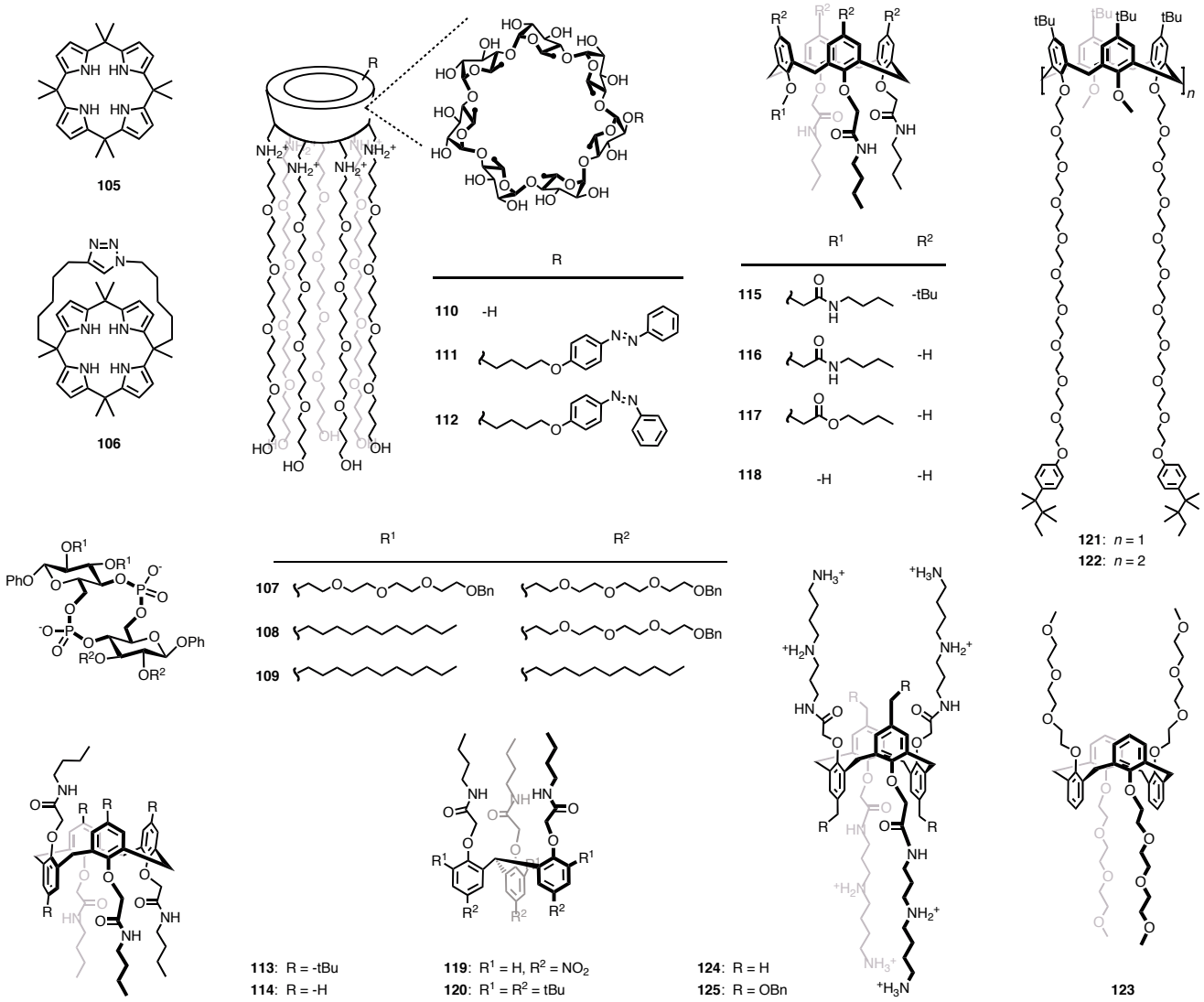

Fig. 10. Recent macrocyclic transporters include calixpyrroles, cyclophosphodiesters, cyclodextrins and various calixarenes.

The attachment of one azobenzene unit at the upper rim of the macrocycle produces a synthetic ion channel that can be gated with light.[80] In the *trans*-channel **111**, inclusion of the matching *trans*-azobenzene within the macrocycle was proposed to account for preferred transport of smaller cations and to hinder the transport of larger anions. Photochemical isomerization into the *cis*-channel **112** was reflected by a loss in ion selectivity that could originate from the release of the azobenzene from the interior of the cyclodextrin macrocycle.

Calixarenes such as **113**-**118** have been explored extensively as synthetic ion channels.[1,2,81] The general idea has been that cation selectivity could be achieved by cation-π interactions within the macrocycle. Calixarenes **113** and **114** are in partial cone conformation (i.e., three up one down).[82] Hydrophobic amide tails are added to assure both the binding of the mcrocycle to the membrane and the binding of anions to the preorganized NH-bonding arrays near the macrocycle. In the lucigenin assay in fluorogenic vesicles, calixarene **113** with additional *tert*-butyl groups was inactive, whereas calixarene **114** without *tert*-butyl groups was active. Structural studies by NMR and X-ray implied that the *tert*-butyl groups destroy the supramolecular organization that is required for anion transport. Intriguingly, the *tert*-butylated calix[4]arene **113** functioned as inhibitor of the supramolecular transporters formed by calixarene **114**. The same observation was made with the series of cone-shaped conformers **115**-**118**, where the introduction of *tert*-butyl groups in **115** removed all transport activity.[83] Substitution of one amide group in **116** by a similarly hydrophobic ester in **117** reduced activity. Replacement by a phenol in **118** introduced pH sensitivity with reduced anion transport activity at high pH, presumably due to charge repulsion. Contraction of calixarene **115** into the acyclic tripod transporter **119** provided access to HNO_3 symport with high selectivity against chloride. To determine this interesting activity, an innovative assay in fluorogenic vesicles had to be developed. Inactivity obtained in response to the substitution

of the nitro groups in **119** by *tert*-butyl groups in **120** pointed toward supramolecular active structures.[84]

Triton X-100 is one of the textbook examples that a simple surfactant known for its destructive impact on lipid bilayers in micellar form can, under optimized conditions, behave like a synthetic ion channel.[1,85] In calix[4]arene **121** and calix[6]arene **122**, both in *cone* conformation with inactivating *tert*-butyl groups at the opposite upper rim, triton X-100 tails were attached to two of the four arenes at the lower rim.[86] In planar bilayer conductance experiments at pH 7, the calix[6]arene **122** yielded homogenous, small and ohmic channels with 26 pS conductance and lifetimes from 0.5 to remarkable 20 seconds. Larger currents, observed particularly at higher concentrations, were interpreted as originating from groups of monomers that open in a cooperative manner. Calix[6]arene **122** was inactive when KCl instead of NaCl was used, and the contracted calix[4]arene **121** was inactive under all conditions. Both effects were explained by obstruction of cation flux through the macrocycle by the bulky *tert*-butyl groups at the upper rim.

The 1,3-*alternate* calix[4]arene **123** was shown by NMR to bind sodium cations.[87] Sodium recognition by cation-π interactions within the macrocycle was supported by computational studies. In planar bilayer conductance experiments, long-lived single channel openings were found in the presence of sodium but not in the presence of potassium cations.

The 1,3-*alternate* calix[4]arenes **124** and **125** with spermidine side chains are polycations in neutral water.[88] Hindrance by additional benzyloxy groups in **125** caused inactivity, the Boc-protected analog of **124** was also less active. Routine analysis with the HPTS assay in vesicles suggested selectivity for anions. The found Hofmeister selectivity sequence implied weak binding of at least partially dehydrated anions during transport. Transport of oxyanions was less important, perchlorate and glutamate inhibited the transport of chloride. Consistent with better transport activity, the debenzylated **124** was more cytotoxic than **125**. Calix[4]arenes were also functionalized with the biological ion channel amphotericin B.[89] This covalent capture of the putative active barrel-stave bundle influenced antifungal activity, hemotoxicity and potassium efflux from ergosterol-rich POPC vesicles.

Oligocrowns **126** and **127** contain a redox active ferrocene unit in the middle and fluorescent anthracene anchors at both termini (Fig. 11).[90] Na NMR assays in vesicles revealed transport activity for both channels, relatively linear Hill plots could support unimolecular active structures. Oxidation of the ferrocene with ceric (IV) ammonium nitrate caused channel inactivation, presumably due to ejection of the charged ferricenium channel from the membrane. Planar bilayer conductance experiments revealed ohmic, homgenous, long-lived and small ion channels. The contracted 5-crown-15 channels **126** showed occasional $Na^+/K^+ \sim 2.5$ selectivity, whereas the expanded 6-crown-18 channels **127** had no Na^+/K^+ selectivity. The open probability, that is the probability to observe an open channel, increased with increasing voltage applied.

Crown ether oligomers such as **128-141**, also referred to as hydraphiles, rank among the oldest synthetic ion channels.[1,2,5] During the period of this review, the activity of the new analogs **128-133** was determined as **130** > **129** > **128** > **131** > **132** > **133** in vesicles composed of DOPC and DOPC/DOPA 7:3 mixtures.[91] A roughly linear dependence on the Hammet substituent constant was considered as support for operational cation-π interactions with the lipid headgroups. The anchoring of aromatics at the membrane-water interface is an ubiquitous phenomena in biological and synthetic ion channels.[1,2,5]

The introduction of amides into the classical oligocrown scaffold **134-136** gave best results for **134** with amides in the periphery ($EC_{50} \sim 12$ μM).[92] Increasing lipophilicity when moving from ammonium cations to neutral amides is likely to account for this increase. Amides **134-136** showed antibiotic activity. Removal of the central crown in **137-140** gave best results for **140**, where amides in the core could assure partitioning and arenes at the termini cation-π anchoring.[93] The same arrangement was successful in **141**, whereas the introduction of calix[4]arene and calix[6]arenes at several positions produced inactive material.[94]

Oligocrowns **142** with a *meta*-phenyldiamide relay were less active than analogs with a central crown, but differences in solubility complicated quantitative comparisons.[95] Further removal of the terminal crowns gave membrane-spanning bolaamphiphile **143** with central amide as anion or cation relay. Bolaamphiphile **143** was reported to mediate the release of large anionic probes from DOPC vesicles with a relatively weak EC_{50} around 50 μM.[96] A Hill coefficient of 1.5 implied that the existence of at least dimeric and unstable active suprastructures. In planar bilayer conductance experiments, long-lived homogenous single channels with weak cation selectivity were observed. The conductance increased with time up to 0.14 nS, corresponding to a pore diameter of > 9.3 Å. Analogs **144** and **145** showed increased activity in vesicles and single-channel currents in planar bilayer conductance experiments.[95]

Crown ethers **146-152** with hydrophobic urea chains form linear stacks with flanking hydrogen-bonded chain in the solid state.[97] In single-channel measurements, all samples showed short-lived irregular bursts except for **149**, which formed longer-lived channels with discrete but variable conductance levels. The single-channel conductance of 29 pS correlated well to the diameter of crown ethers.

Ion channels formed by cyclodextrin polymers will be described in chapter 3.8 on polymers, peptide crown hybrids and peptide macrocycles in the following chapter.

3.7 Peptide mimics

Inspired by biological examples such as valinomycin or the gramicidins, macrocyclic peptides and peptide mimics have been explored extensively as synthetic transport systems.[98] During the period of this review, the cyclopeptoids **153-156** were tested for cation transport activity (Fig. 12).[99] Compared to cyclopeptides, cyclopeptoids are attractive because the absence of NH hydrogen bond donors should prevent anion binding and the self-assembly into supramolecular active

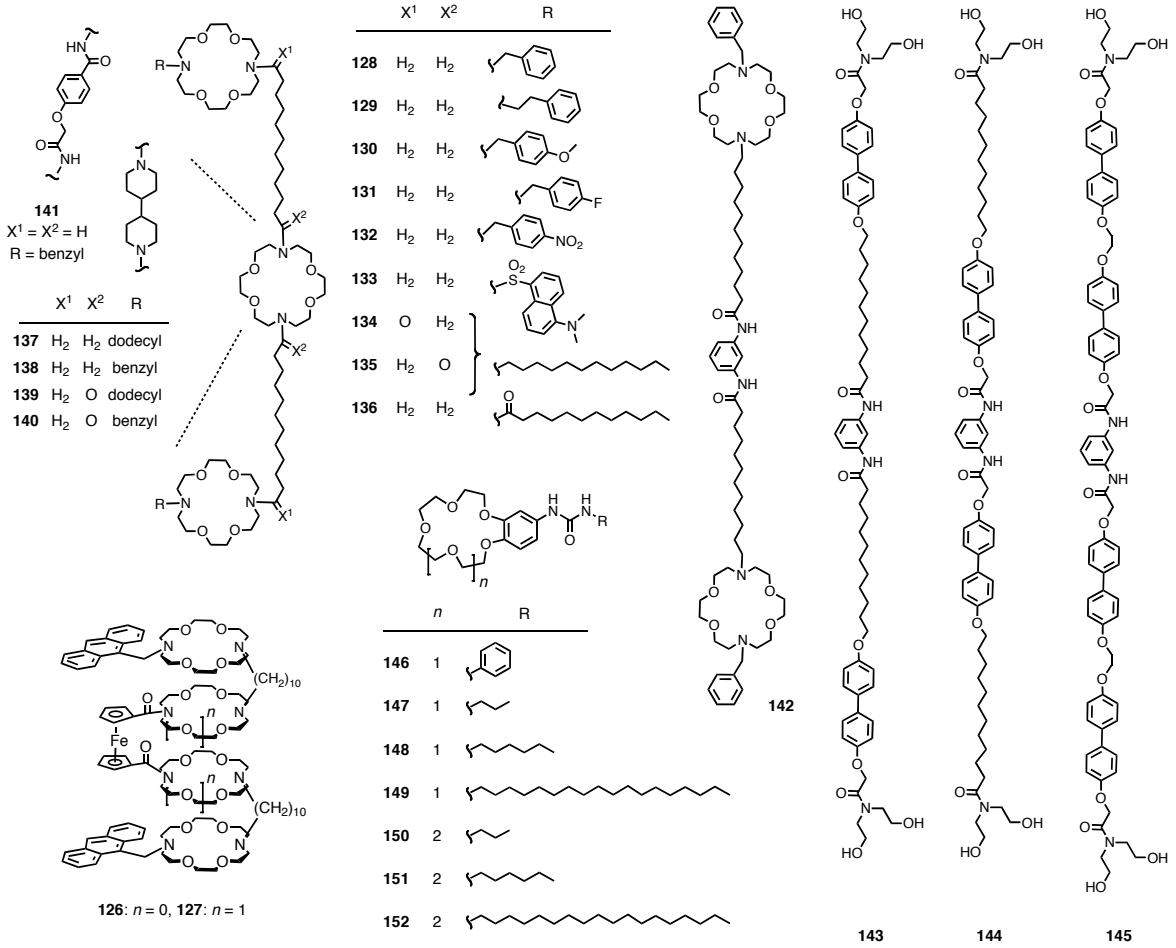

Fig. 11. Recent macrocyclic transporters also include crown ethers.

structures. The flexible eighteen-membered *N*-benzyloxyethyl macrocycle **154** was known to strongly bind small cations such as Li^+, Na^+ and K^+ in the focal point of the preorganized carbonyl ligands. Picrate extractions in bulk membranes confirmed that the expanded cyclopeptoids **155** and **156** preferred larger cations. In fluorescently labeled 95:5 EYPC/EYPG vesicles, the contracted macrocycle **154** transported Na^+ with high selectivity, whereas the expanded macrocycle **155** showed $Cs^+ > Rb^+ > K^+$ selectivity. Linear Hill plots could suggest that cyclopeptoids act as unimolecular ion carriers without higher order active structures. The extreme macrocycles **153** and **156**, either too small or too floppy, were both inactive.

Aromatic oligoamides **157** and **158** are the first members of a family of carefully crafted, shape-persistent, planar macrocycles[100] that form ion channels in lipid bilayers.[101] As with peptoids **153-156**, carbonyl ligands could be expected to bind cations in the middle of the macrocycle, whereas hydrophobic peripheral tails at the periphery could interact well with the surrounding membrane. Different to peptoids **153-156**, π-π interactions between macrocycles **157** and **158** could drive the self-assembly into transmembrane stacks that could act as barrel-hoop cation channels. Linear Hill plots obtained from Na NMR assays in vesicles suggested that **157** acts as monomer or stable supramolecule. Single channel measurements gave ohmic and homogenous conductance levels for both **157** and **158**. Hille analysis of their 890 pS conductance gave values that are compatible with the large inner diameter of ~8.3 Å of π-stacked macrocycles **157** and **158**.

Self-assembling macrocyclic urea/amide hybrids[102] have been introduced as functional, anion-selective transporters in lipid bilayer membranes.[103] In macrocycles **159-164**, the side chains (aliphatic and aromatic) and conformations (amplified or annihilated carbonyl dipoles) are varied. With EC_{50}s ~ 3 μM, aromatic macrocycles **159-161** were much more active than their aliphatic analogs **162-164** (EC_{50}s ~ 60 μM). This difference was as expected from the preferred partitioning and translocation of aromatic residues.[1,2] Anion transport by macrocycles **159** and **160** exhibited anti-Hofmeister and Hofmeister selectivity, respectively. This dichotomic behavior coincided with the self-assembly of macrocycles **159** / **160** into nanotubes with / without macrodipole, respectively. Strong anion binding by anti-Hofmesiter macrocycles **159** was thus likely to occur at the positive end of the nanotube by macrodipole-anion interactions. Ubiquitous in biology,[22] this is the first application of macrodipole-anion interactions in synthetic transporters. Voltage-sensitivity was expressed *inter alia* as decreasing Hill coefficients of **159** (but not the dipole-free **160**) with membrane polarization. This finding

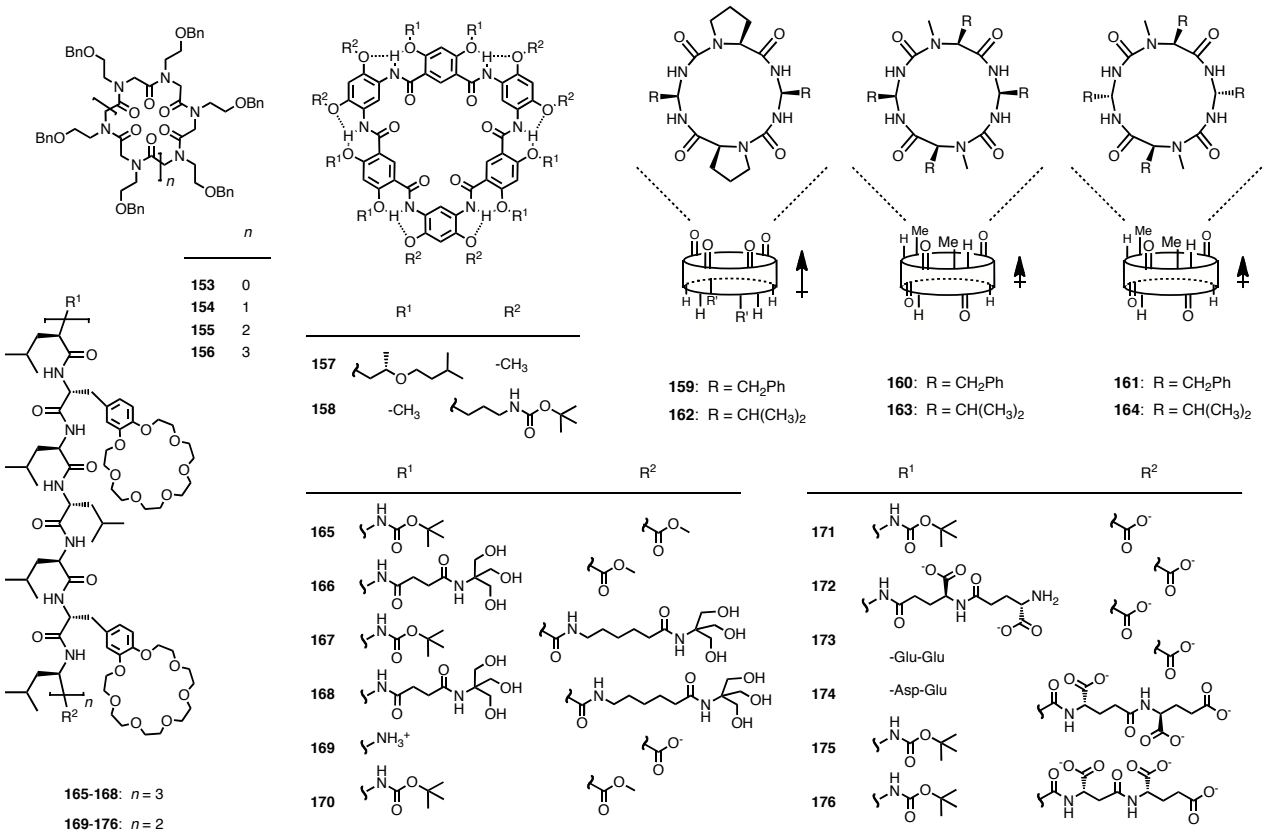

Fig. 12. Peptide mimics as synthetic transport systems.

suggested that the nanotubes formed by **159** are stabilized by macrodipole-potential interactions. With the internal space of nanotubes formed by self-assembled **159** being much too small to let anions pass through, a new transport mechanism was proposed to explain the results, where individual macrocycles in a transmembrane stack rotate around their own axis like in a "Jacobs ladder" to hand over anions without moving themselves.

Hydrophobic peptides with crown-ether side chains aligned one on top of the other along an α-helical scaffold have been studied for more than a decade by now.[104] Most recently, emphasis has been on end group engineering of membrane-spanning 21-mers **165-168**.[105] Best sodium transport activity was found for peptide **166** with a hydrophilic TRIS motif at the N-terminus to increase delivery to the membrane and perhaps also facilitate partitioning and orientation. Anionic amino acids at one or both ends of the shorter 14-mers **169-176** caused high calcein leakage from 7:3 DOPC/cholesterol vesicles.[106] Leakage activity decreased in the order **169 ~ 171 ≥ 175 ~ 176 >> 173 > 174 > 172 > 170**.

Peptide-lipid hybrids **177-198** are constructed around a G_3PG_3 motif that is anchored in the membrane with two hydrophobic termini (Fig. 13).[107-117] Because it occurs in biological chloride channels, the G_3PG_3 motif has been suggested to introduce chloride selectivity. Chloride efflux has indeed been detectable with chloride-selective electrodes in the past. However, coinciding efflux of larger probes such as CF occurred at similarly high μM concentrations, and the extent of selectivity remains largely obscure. During the period of this review, extensive structure-activity relationship studies have been reported.[107-117] Modification of the number of glycines and of the position of the proline in peptides **177-181** suggested that the lengthening of the peptide and the shifting of the proline residue towards the C-terminus increases transport activity.[108] The G_3PG_3 peptide **177** had an EC_{50} ~ 45 μM, best activities were found for the elongated G_4PG_4 analog **181**. The Hill plot for CF leakage from fluorogenic vesicles showed a Hill coefficient n = 1.4, suggesting that the active structure is, at least, an unstable dimer.

In the series **182-187**, the original C (benzyl) and N (octadecyl) terminal groups are varied.[112] The activity sequence **186** >> **182** ~ **185** > **184** ~ **183** ~ **177** correlated well when using a chloride selective electrode and a lucigenin-based vesicle assay, whereas a slightly different trend was found for CF release (**182** > **185** > **184** > **177** > **186** > **183**). Judged from single-point data, overall activities were rather weak. In U-tube experiments, **177** and **182** showed KCl-dependent CF transport activity. This finding was interpreted as evidence against a carrier mechanism for CF transport.

It was also reported that the presence and the position of positively or negatively charged amino acids such as lysine and glutamate in peptide transporters **188-194** diminishes transport activity.[110,114,115] For the anionic peptides **189**, **191** and **193**, simple charge-charge repulsion could account for the inhibition of anion efflux. The transport activity of lysine peptide **194** depended of lipid composition of the vesicles.

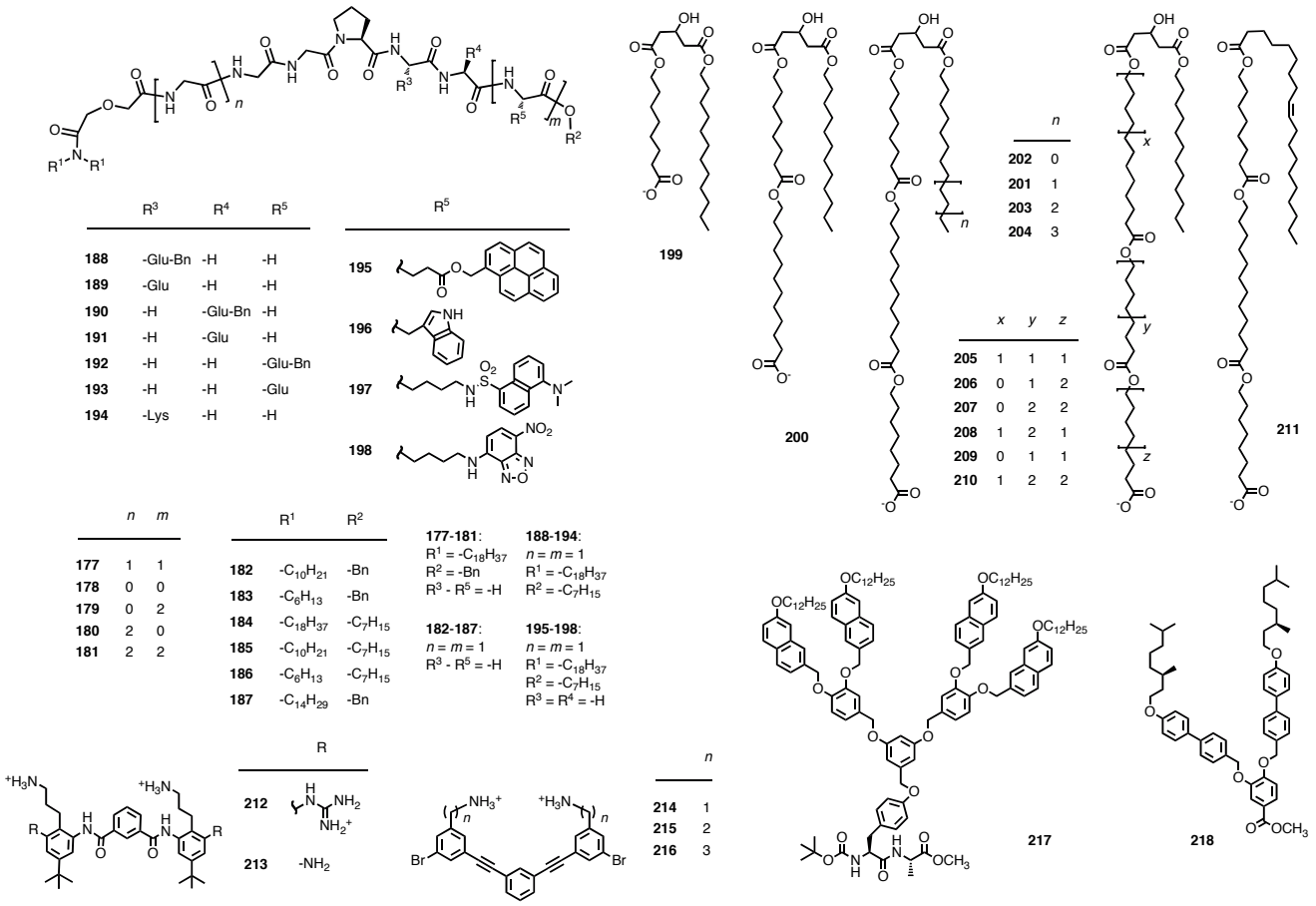

Fig. 13. More peptide mimics as synthetic transport systems.

This finding suggested that the positively charged peptide could disrupt important interactions in the membrane that lead to the formation and function of the pore. In vesicles, best activities were found for the neutral peptide **192**. In planar bilayer conductance experiments, homogenous ohmic channels with a conductance of 29.8 pS were reported for the anionic peptide **193**.

Fluorescent analogues **195-198** were used to study the assembly of these peptides in the bulk phase and in the lipid bilayer.[116] FRET experiments with compounds **195** and **196** were used to prove aggregate disassembly in the transition of the probe going from the buffer to the lipid membrane. The pyrene derivative **195** was the most active analog at 65 μM. It showed excimer emission in buffer but not in vesicles.

Oligoester transporters have a long tradition as bioinspired peptide mimics.[1,2,118] Linear oligoester amphiphiles such as **199-211** have been prepared as part of an effort to simplify complex architectures of the original synthetic ion channels (Fig. 14).[119-121] An elegant solid-phase synthesis approach was conceived to rapidly produce large libraries. As most active members of a small collection, dimer **199** showed high activity in vesicles.[119] Trimer **200** and tetramer **201** were already less active. The linear Hill plots indicated the presence of a unimolecular or a stable supramolecular active structure.

On the basis of Amphiphile **201**, the ester position as well as the length of the alkyl segments was systematically changed. [121] In the HPTS assay, the amphiphiles **201-211** gave EC_{50}s in the range from 7 μM to 56 μM. Replacement of the hydroxy group with a *cis*-alkene in **211** did not cause dramatic changes in activity. More hydrophilic amphiphiles with extended lengths close to the membrane thickness were best ones. Micelle formation of oligoester amphiphiles in the aqueous media was confirmed to be a rate-limiting step in transport experiments with fluorescently-labeled vesicles.

The facial amphiphiles **212-216** have been studied extensively as minimalist mimics of antibiotic peptides such as magainin.[122-128] Several lines of evidence suggest that they act like their biological counterparts as lipid-dependent micellar pores in biomembranes as well as biomembrane models.

Dendritic dipeptides such as **217** are known to self-assemble in the solid state into barrel rosette architectures.[129] Their hydrophobic pores, conceived as reminiscent of the interior of carbon nanotubes on one hand and biological water channels, i.e. aquaporins, on the other hand, were suggested as

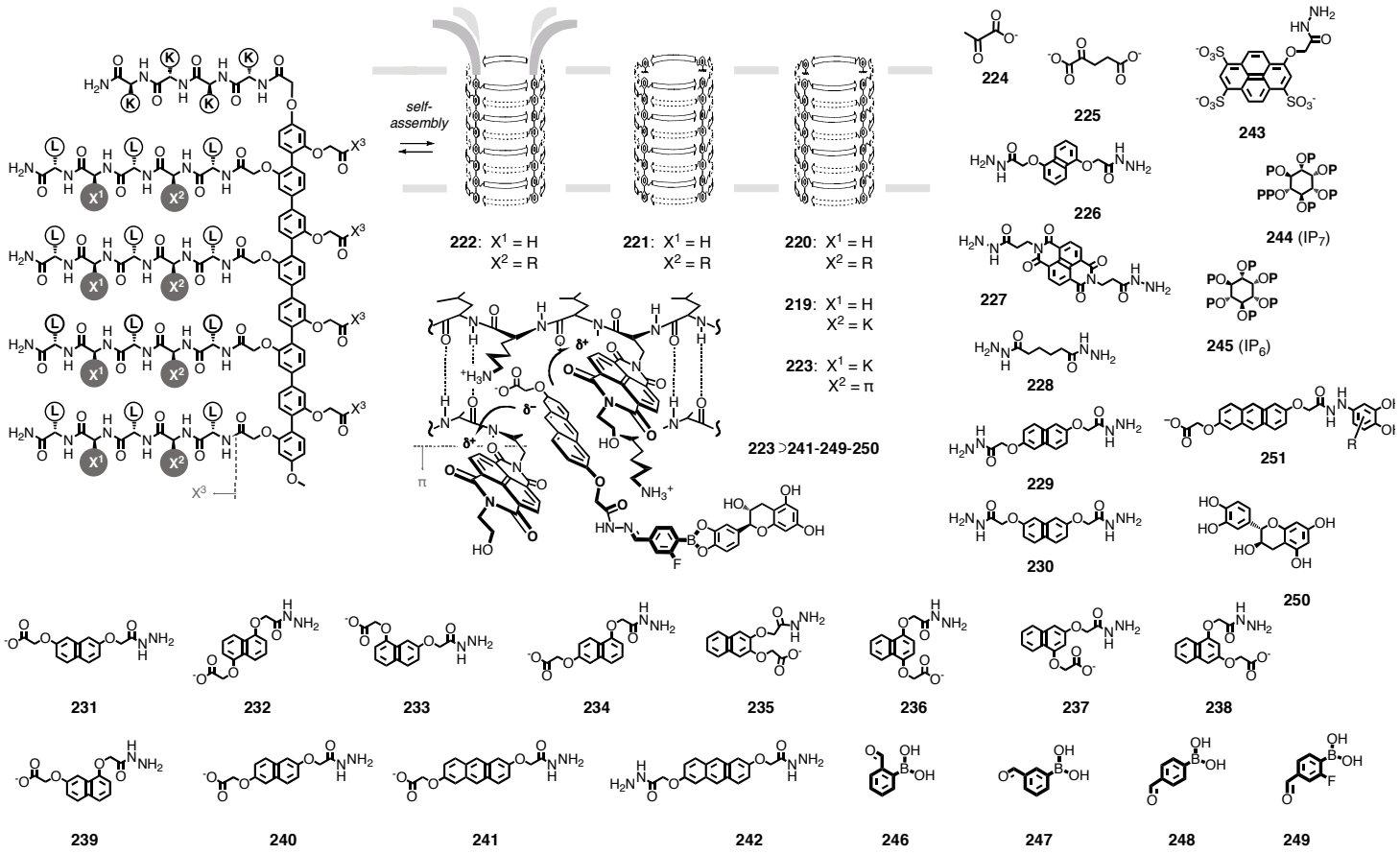

Fig. 14. Recent synthetic pore sensors made by artificial β-barrels **219**-**223**, together with analytes, signal amplifiers and signal converters. Single letter amino acid abbreviations.

ideal to transport water selectively. This topic is of interest for the development of innovative water purification systems.

To detect water transport, peptides **217** were added to GUVs (giant unilamellar vesicles), and their response to the aspiration by a micropipette was measured on the microscope. Possibly accelerated GUV relaxation in the presence of peptide **217** was interpreted as facilitated water release from the GUV interior to an external hypertonic solution. Inactivity in all control experiments was interpreted as selectivity. Similar but clearly not identical CD spectra in solid state and lipid bilayers were proposed as support for the formation of barrel-rosette architectures in the latter.

The same dendritic peptide **217** and the peptide-free dendron **218** were incorporated into poly(ethylene oxide)-polybutadiene (PEO-PBD) polymersomes, i.e., vesicles made from amphiphilic polymers rather than from lipids.[130] In proton transport experiments, the peptide-free dendrons **218** were clearly more active than the dipeptide dendrimers **217**, suggesting that the peptide moiety is irrelevant for function. This is one of the few synthetic transport systems that have been characterized in polymersomes.

Artificial β-barrels such as **219** or **220** composed of *p*-octiphenyl staves as shape-persistent 3D turns between short β-sheets have been reported first in 1999 (Fig. 14).[1,2] Progress made during the current period concerns modifications of staves,[131] termini[132] and internal active sites[133,134] as well as covalent capture approaches for signal amplification in sensing applications.[135-141] As far as the stave are concerned, replacement of the $1^3,2^3,3^2,4^3,5^2,6^3,7^2,8^3$-pattern in **220** with a regioisomeric $1^2,2^2,3^3,4^2,5^3,6^2,7^3,8^2$-motif in **221** did not disturb the formation of multifunctional β-barrel pores.[131] Attachment of tetralysine (K_4) tails in **222** improved pore delivery to the membrane.[132] An increase in the Hill coefficient from $n = 1$ for **221** without K_4-tails to $n = 4$ for **222** with K_4-tails suggested that charge repulsion between the K_4-tails causes the desired destabilization of the active tetramer.

The construction of β-barrel mimics with artificial amino acids contributing to the internal active sites was achieved in supramolecule **223**.[133,134] The π-acidic NDI side chains were introduced to act as internal π-clamps or tweezers and form charge-transfer complexes with π-basic blockers. The obtained pores were tetrameric, unstable but inert, acid-insensitive but sensitive to base and ionic strength. The contribution of the internal π-clamps to molecular recognition was assessed by comparison of pore blockage efficiencies with pore **219**, where π-clamps are replaced by histidines. Purine nucleotides were better recognized with a π-clamping factor up to 9.6 for AMP.

Decreasing ionic strength revealed decreasing π-clamping factors at increasing affinities down to an IC_{50} = 14 μM for ATP and an IC_{50} = 22 μM for GTP, respectively. Formal double mutant cycles were established with hydrazone blockers formed from pyruvate **224** and α-ketoglutarate **225** reacted with π-basic dihydrazide **226**, π-acidic dihydrazide **227** and aliphatic dihydrazide **228**. The blockage efficiency with π-basic blockers increased 40-fold from pore **219** to pore **223** with IC_{50} = 240 nM, whereas that with π-acidic blockers increased only 10-fold to IC_{50} = 2.5 μM, which adds up to a factor of four for the isolate contribution from aromatic electron donor-acceptor (AEDA) interactions.[134] Aliphatic hydrazone controls obtained from **228** and **225** did not inactivate pore **223** at all. The efficiency of hydrazones formed by α-ketoglutarate **225** and π-basic dialkoxynaphthyl regioisomers **229**-**240** to inactivate pore **223** increased from 2,7-isomer **231** with IC_{50} = 15 μM to 2,6-isomer **240** with IC_{50} = 6.5 μM.[135] The found trends could be explained by improved π-clamping due to decreasing oxidation potentials from $E_{1/2}$ = 1.16 V (**231**) to $E_{1/2}$ = 0.91 V (**240**), increasing quadrupole moments from Q_{ZZ} = -11.9 B (**231**) to Q_{ZZ} = -13.2 B (**240**) and, most importantly, the matching of overlapping HOMO and LUMO orbitals. These lessons learned were applied in the design of anthracene blocker **241**, where further maximized $E_{1/2}$ = 0.71 V and Q_{ZZ} = -15.7 B and preserved matching of HOMO and LUMO orbitals resulted in IC_{50} = 300 nM for the corresponding hydrazone blocker. The complementary dihydazone blockers **229**, **230** and **242** gave the same trends. These results suggested that the π-acidic π-clamp in pore **223** catches the π-basic intercalators in a twisted orientation.

For sensing applications, hydrazide blockers are of interest as signal amplifiers. With pyrenetrisulfonate hydrazide **243** to covalently capture the products of enzymatic signal generation, pore **219** could sense lactate, citrate and glutamate (umami) in food samples from the supermarket.[136] Consumption of ATP blockers was sufficient to sense sucrose, lactose or acetate with pore **219** as signal transducer and kinases for signal generation.[136] Sensing of IP_7 **244**, phytate **245** and lower inositol phosphates was possible without signal amplifiers or co-substrate, also in beans or almonds.[137] Enantiomer discrimination was explored for α-helices and lactate with pore **219** and the aid of proteases and lactate oxidase as enantioselective signal generators.[138,139] Signal amplification of analytes other than ketones or aldehydes was exemplified with the reaction of hydrazides such as **241** with aldehydes **246**-**249**.[140] Inactivation of pore **223** with the resulting boronic acids could be reversed by covalent capture of catechols such as catechin **250** or epigallocatechin gallate. To also sense catechol-free polyphenols such as resveratrol in red wine, tyrosinase was used as signal generator. The obtained reactive *ortho*-quinones were directly captured with hydrazide **241** to give pore blockers such as **251**.[141]

3.8 Synthetic polymers

Synthetic polymers and biopolymers have been studied as transporters in bilayer membranes in many variations. This research overlaps substantially with biomedical and bioengineering topics such as antimicrobials or drug delivery. In many cases, evidence for transport activity is indirectly implied from cellular uptake experiments, characterization in vesicles is often simply skipped. The coverage in this review is thus necessarily less comprehensive compared to other chapters, specific topics are constantly reviewed from different points of view.[13,14,20]

Polymer transporters are usually conceived as polymerized amphiphiles. Also referred to as amphipols, such amphiphiles have been introduced originally as macromolecular detergents or "covalent micelles" to solubilize membrane proteins.[142] However, their ability to form ion channels and pores in lipid bilayers has been recognized early on.[1,2,13] During the covered period, polyacrylate **252** was shown to form pH-gated pores in calcein-loaded vesicles (Fig. 15).[143] pH Gating was rationalized as coil-to-globule conformational change above pH 7. Recent examples for membrane-active graft copolymer pores include polyanionic **253**.[144] Variation of the composition of copolymer **254** with hydrophobic acrylamides and anionic polyacrylates revealed that increasing negative charges yield better activity, whereas only small fractions of hydrophobic tails is needed for transport activity.[145] Amphipol **255**, composed of hydrophilic polyacrylate together with alkyl and aryl polyacrylamide, was shown to generate in part very large single-channel current in planar bilayers.[146] Conductance of up to 4.3 nS and the release of vesicle-entrapped fluorescently labeled dextrans were both consistent with the formation of giant pores with inner diameters up to 4 nm. Polyacrylate **256** with glycerostearyl tails was shown to form pores in polymersomes.[147] This finding was of interest because only few studies exist on the activity of synthetic transport systems in polymersomes.[130,147] Coil-to-globule transition of polyacrylate **256** in the pH range from 5.0 to 8.0 induces content release from the polymersome.

Ion channels **257** and **258** feature polyethyleneglycol (PEG) tails grown on amphiphilic β- or γ-cyclodextrin macrocycles, respectively.[148] Ohmic, homogenous and very long-lived ion channels were observed in planar bilayer conductance experiments. Unexpectedly small ion channel diameters around 1 Å increased slightly with increasing diameter of the macrocycle as well as with increasing concentrations. High activity with double-sided addition suggested that macrocycles are needed to form active ion channels that span the bilayer membrane.

Cationic amphiphiles such as steroids, peptides, peptide mimics and amphipols such as **259**-**260** are extensively explored in search for new antimicrobials.[149-161] Studies usually focus directly on the determination of antibiotic activity compared to hemolytic activity as a measure for toxicity. In most cases, it is assumed that recognition and permeabilization of the anionic, negatively polarized, microdomain containing bacterial membranes account for this activity. In some cases, studies in model membranes are reported. The release of fluorescent probes from neutral POPC vesicles was considered as similar to hemolytic activity, i.e., toxicity. With polymers **259**-**260**, for example, activities increased with increasing hydrophobicity.[155] Activity in anionic POPE/POPG and DOPG/lysyl-

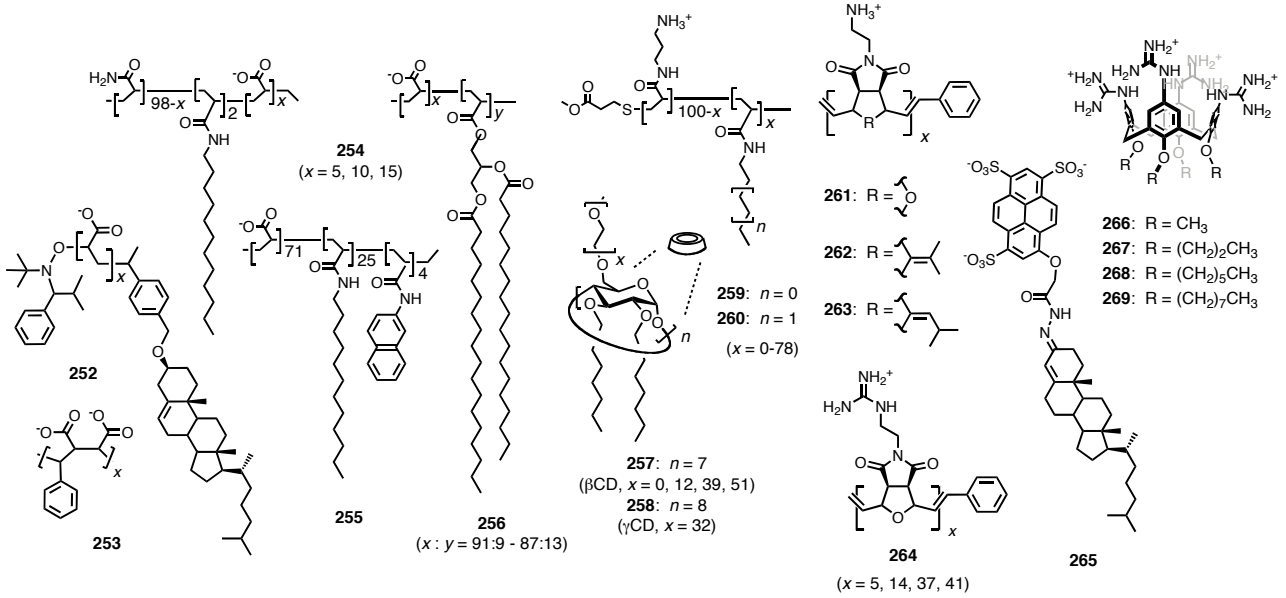

Fig. 15. Synthetic transport systems made from polymers **252-264** and/or activators of polyion-counteiron transport systems such as **265-269**.

DOPG/cardiolipin vesicles was considered as indicative for antibiotic activity. Cationic homopolymers caused gradual dye release, the more hydrophobic copolymers caused rapid efflux.

The cationic polynorbornenes **261-264** are of interest as antimicrobials and to mediate cellular uptake.[159] They are obtained by ring-opening olefin metathesis polymerization of amphiphilic monomers.[159-161] The ability of polynorbornenes **261-263** to accelerate dye release from fluorogenic vesicles increased with increasing hydrophobicity of the tails opposite to the cationic ammonium head groups.[160] Studies by isothermal titration calorimetry, dynamic light scattering and fluorescence microscopy indicated that polynorbornenes **261-263** cause extensive vesicle aggregation without complete bilayer disintegration.

Polyguanidino-oxanorbornenes **264**, also referred to as PGONs, were identified as anion transporters in lipid bilayers that respond to chemical stimulation.[161] PGON transporters **264** were most active in neutral bilayers near their phase transition. Best EC_{50}s were in the nanomolar range. Negative surface potentials reduced and inside-negative membrane potentials increased activity. The activity of polyguanidino-oxanorbornenes **264** increased with polymer length in a non-linear manner. Their activity increased slightly in the presence of amphiphilic anions such as pyrenebutyrate (EC_{50} = 70 μM) and decreased in the presence of hydrophilic anions such as ATP, ADP, heparin or phytate. A fluorogenic lactate biosensor was constructed to illustrate compatibility of PGONs **264** with multicomponent sensing in complex matrices such as milk serum.

The role of counterions to regulate the activity of biological and synthetic polyions in lipid bilayers continues to attract intense scientific attention for several different reasons. This includes the voltage gating of biological potassium channels[18] or counterion-mediated cellular uptake of polyanions such as DNA or RNA[20] or polycations such as the arginine-rich CPPs.[19] A comprehensive review of intense research on cationic amphiphiles for the cytosolic delivery of RNA or DNA is beyond the scope of this review, also because the characterization of the functional polyion-counterion systems as transporters in lipid bilayer membranes is often missing.[20,162-164] Recent progress with polyion-counterion transporters in fluorogenic vesicles includes their use to detect the activity of enzymes in new enzyme assays[165] and to sense cholesterol after enzymatic oxidation and covalent capture as amphiphile **265**.[166] Moreover, countercations such as amphiphilic calixarenes **266-269** (but not their bolaamphiphilic *1,3-alt* conformers) have been introduced to activate DNA as cation transporters in bulk and bilayer membranes.[167,168] Based on this breakthrough, counterion-activated DNA aptamers have been introduced as combined, universal signal generators and signal transducers in membrane based sensing systems.[169]

4 Epilogue

Over the last four years, another great collection of synthetic transport systems has appeared in the literature. Established motifs have been refined, new architectures have been introduced. It is safe to say that the simple punching of holes in membranes does not pose significant problems anymore. Fundamental studies on structure-activity relationships fully confirm this conclusion and, although highly valuable and important, have to pay attention not to become repetitive. The same holds for the introduction of new architectures that do not go beyond simple transport. What arguably matters most is conceptual innovation. Gratifyingly, there has been plenty of it during the past four years. Innovative architectures such as "heavy-metal" systems, π-stacks and calix[4]pyrrole, phosphodiester, peptoid, arylamide or urea/amide macrocycles

are remarkable, highly creative contributions (Figs. 4, 5, 8 and 9). The introduction of either very weak or new interactions for anion transport marks another emerging, highly innovative trend with possible importance well beyond the topic (e.g., organocatalysis, cellular uptake). Realized examples cover phthalic diamides, catechols, urea lipids, anion-π interactions, anion-macrodipole interactions, charge-transfer complexes or "dynamic" polyion-counterion pairing (Figs. 6, 7, 9, 14, 15). Conceptually new transport systems that respond to light or chemical stimulation have been realized in many variations, including organometallic and dynamic covalent chemistry. As far as applications are concerned, conceptually important contributions cover topics such as activity in live cells (ion channel regulation, antibiotic activity, cellular uptake) and the construction of new sensors. This exciting recent progress justifies highest expectations for the years to come.

5 Acknowledgments

We thank all authors of unintentionally overlooked contributions for accepting our sincere apologies, L. Babel for contributions to literature search, and the University of Geneva, the Swiss National Science Foundation (NSF), the National Centre of Competence in Research (NCCR) in Chemical Biology, and the European Research Council (ERC, Advanced Investigator) for financial support.

Abbreviations

ADP, adenosine-5'-diphosphate; AMFE, anomalous mole fraction effect; AMP, adenosine-5'-monophosphate; TRPA, transient receptor potential ankyrin; ATP, adenosine-5'-triphosphate; CD, circular dichroism; CF, 5(6)-carboxyfluorescein; CPP, cell-penetrating peptide; CSA, cationic steroid antibiotic; DNA, deoxyribonucleic acid; DOPA, dioleoyl phosphatidic acid (PA, 1,2-diacyl-*sn*-glycero-3-phosphate); DPPC, dipalmityl phosphatidylcholine (1,2-diacyl-sn-glycero-3-phosphocholine); DPPG, dipalmityl phosphatidylglycerol {1,2-diacyl-sn-glycero-3-[phospho-*rac*-(1-glycerol)]}; POPC, 1-palmitoyl-2-oleoyl phosphatidylcholine; DOPC, dioleoyl phosphatidylcholine; DOPE, dioleoyl phosphatidyl-ethanolamine (PE, 1,2-diacyl-*sn*-glycero-3-phosphoethanolamine); DOPG, dioleoyl phosphatidylglycerol; EC_{50}, effective concentration; EYPC, egg yolk phosphatidylcholine; EYPG, egg yolk phosphatidylglycerol; FCCP, carbonylcyanide 4-(trifluoromethoxy)phenylhydrazone; FRET, Förster (fluorescence) resonance energy transfer; G, glycine / guanosine; G quartet, guanosine quartet; GUVs, giant unilamellar vesicle; GTP, guanosine-5'-triphosphate; HOMO, highest occupied molecular orbital; HPTS, 8-hydroxy-1,3,6-pyrenetrisulfonate; IC_{50}, inhibitory concentration; LUMO lowest unoccupied molecular orbital; LUV, large unilamellar vesicle; MOF, metal-organic framework; MOP, metal-organic polyhedron; NDI, naphthalenediimide; NMR, nuclear magnetic resonance; O-NDI, oligo-NDI; O-PDI, oligo-PDI; P, proline; PAMAM, poly(amido amine); PBD, polybutadiene; PEG, poly(ethylene glycol); PEO, poly(ethylene oxide); PDI perylenediimide; PGON, polyguanidino-oxanorbornene; POPE, 1-palmitoyl-2-oleoyl phosphatidylethanolamine; POPG, 1-palmitoyl-2-oleoyl phosphatidylglycerol; RCM, ring-closing olefin metathesis; RNA, ribonucleic acid; TNT, 2,4,6-trinitrotoluene.

TOC:

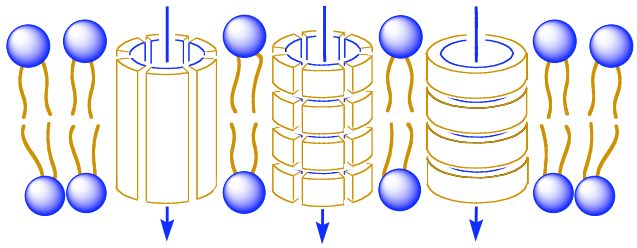

A comprehensive overview of the last four year's creations is provided, highlighting milestone achievements such as the introduction of "heavy-metal" and π-π architectures, or the generation of function with metal-organic, anion-π and anion-macrodipole interactions.

6 References

1 S. Matile, A. Som and N. Sordé, *Tetrahedron*, 2004, **60**, 6405-6435.
2 A. L. Sisson, M. R. Shah, S. Bhosale and S. Matile, *Chem. Soc. Rev.*, 2006, **35**, 1269-1286.
3 T. M. Fyles, *Chem. Soc. Rev.*, 2007, **36**, 335-347.
4 A. P. Davis, D. N. Sheppard and B. D. Smith, *Chem. Soc. Rev.*, 2007, **36**, 348-357.
5 G. W. Gokel and N. Barkey, *New J. Chem.*, 2009, **33**, 947-963.
6 N. Sakai and S. Matile, *Angew. Chem. Int. Ed.*, 2008, **47**, 9603-9607.
7 S. Bhosale, A. L. Sisson, N. Sakai and S Matile, *Org. Biomol. Chem.*, 2006, **4**, 3031-3039.
8 J. Mareda and S. Matile, *Chem. Eur. J.*, 2009, **15**, 28-35.
9 J. T. Davis, O. Okunola and R. Quesada, *Chem. Soc. Rev.*, 2010, **39**, 3843-3862.
10 P. A. Gale, *Chem. Soc. Rev.*, 2010, **39**, 3746-3771.
11 S. Licen, F. De Riccardis, I. Izzo and P. Tecilla, *Curr. Drug Discov. Technol.*, 2008, **5**, 86-97.
12 N. Sakai, J. Mareda and S. Matile, *Acc. Chem. Res.*, 2008, **41**, 1354-1365.
13 W. H. Binder, *Angew. Chem. Int. Ed.*, 2008, **47**, 3092-3095.
14 C. Tribet and F. Vial, *Soft Matter*, 2008, **4**, 68–81.
15 S. Matile and N. Sakai, *The Characterization of Synthetic Ion Channels and Pores.* In *Analytical Methods in Supramolecular Chemistry*, C. A. Schalley, Ed., Wiley, Weinheim, 2007, 391-418.
16 L. J. Macpherson, A. E. Dubin, M. J. Evans, F. Marr, P. G. Schultz, B. F. Cravatt and A. Patapoutian, *Nature*, 2007, **445**, 541-545.
17 T. Takeuchi, M. Kosuge, A. Tadokoro, Y. Sugiura, M. Nishi, M. Kawata, N. Sakai, S. Matile and S. Futaki, *ACS Chem. Biol.*, 2006, **1**, 299-303.
18 D. Schmidt, Q. X. Jiang and R. MacKinnon, *Nature*, 2006, **444**, 775-779.
19 N. Sakai and S. Matile, *J. Am. Chem. Soc.*, 2003, **125**, 14348-14356.
20 S. Bhattacharya and A. Bajaj, *Chem. Commun.*, 2009, 4632-4656.
21 X. He, J. Lobsiger and A. Stocker, *Proc. Natl. Acad. Sci. USA*, 2009, **106**, 18545-18550.
22 R. Dutzler, *FEBS Lett.*, 2004, **564**, 229-233.
23 A. K. Hirsch, F. R. Fischer and F. Diederich, *Angew. Chem. Int. Ed.*, 2007, **46**, 338-352.
24 A. Berkessel, N. Gasch, K. Glaubitz and C. Koch, *Org. Lett.*, 2001, **3**, 3839-3842.
25 A. Berkessel, B. Koch, C. Toniolo, M. Rainaldi, Q. B. Broxterman and B. Kapstein, *Biopolymers*, 2006, **84**, 90-96.
26 D. R. Kelly and S. M. Roberts, *Chem. Commun.*, 2004, 2018-2020.
27 B. L. Schottel, H. T. Chifotides and K. R. Dunbar, *Chem. Soc. Rev.*, 2008, **37**, 68-83.
28 P. Gamez, T. J. Mooibroek, S. J. Teat and J. Reedijk, *Acc. Chem. Res.*, 2007, **40**, 435-444.
29 O. B. Berryman, V. S. Bryantsev, D. P. Stay, D. W. Johnson and B. P. Hay, *J. Am. Chem. Soc.*, 2007, **129**, 48-58.
30 D. Quinonero, C. Garau, C. Rotger, A. Frontera, P. Ballester, A. Costa and P. M. Deya, *Angew. Chem. Int. Ed.*, 2002, **41**, 3389-3392.

31 M. Mascal, A. Armstrong and M. D. Bartberger, *J. Am. Chem. Soc.*, 2002, **124**, 6274-6276.
32 I. Alkorta, I. Rozas and J. Elguero, *J. Am. Chem. Soc.*, 2002, **124**, 8593-8598.
33 G. Gil-Ramírez, E. C. Escudero-Adán, J. Benet-Buchholz and P. Ballester, *Angew. Chem. Int. Ed.*, 2008, **47**, 4114-4118.
34 G. Cavallo, P. Metrangolo, T. Pilati, G. Resnati, M. Sansotera and G. Terraneo, *Chem. Soc. Rev.*, 2010, **39**, 3772-3783.
35 P. Auffinger, F. A. Hays, E. Westhof and P. S. Ho, *Proc. Natl. Acad. Sci. USA*, 2004, **101**, 16789-16794.
36 P. Metrangolo, Y. Carcenac, M. Lahtinen, T. Pilati, K. Rissanen, A. Vij and G. Resnati, *Science*, 2009, **323**, 1461-1464.
37 A. Mele, P. Metrangolo, H. Neukirch, T. Pilati and G. Resnati, *J. Am. Chem. Soc.*, 2005, **127**, 14972-14973.
38 T. M. Fyles and C. C. Tong, *New J. Chem.*, 2007, **31**, 655-661.
39 C. P. Wilson and S. J. Webb, *Chem. Commun.*, 2008, 4007-4009.
40 A. Satake, M. Yamamura, M. Oda and Y. Kobuke, *J. Am. Chem. Soc.*, 2008, **130**, 6314–6315.
41 M. Jung, H. Kim, K. Baek and K. Kim, *Angew. Chem. Int. Ed.*, 2008, **47**, 5755-5757.
42 O. V. Kulikov, R. Li and G. W. Gokel, *Angew. Chem. Int. Ed.*, 2009, **48**, 375-377.
43 R. Li, O. V. Kulikov and G. W. Gokel, *Chem. Commun.*, 2009, 6092-6094.
44 M. S. Kaucher, W. A. Harrell Jr and J. T. Davis, *J. Am. Chem. Soc.*, 2006, **128**, 38-39.
45 L. Ma, M. Melegari, M. Colombini and J. T. Davis, *J. Am. Chem. Soc.*, 2008, **130**, 2938-2939.
46 L. Ma, W. A. Harrell and J. T. Davis, *Org. Lett.*, 2009, **11**, 1599-1602.
47 A. Hennig and S. Matile, *Chirality*, 2008, **20**, 932-937.
48 N. Sakai, Y. Kamikawa, M. Nishii, T. Matsuoka, T. Kato and S. Matile, *J. Am. Chem. Soc.*, 2006, **128**, 2218-2219.
49 S. Bhosale, A. L. Sisson, P. Talukdar, A. Fürstenberg, N. Banerji, E. Vauthey, G. Bollot, J. Mareda, C. Röger, F. Würthner, N. Sakai and S. Matile, *Science*, 2006, **313**, 84-86.
50 V. Gorteau, G. Bollot, J. Mareda, A. Perez-Velasco and S. Matile, *J. Am. Chem. Soc.*, 2006, **128**, 14788-14789.
51 V. Gorteau, G. Bollot, J. Mareda and S. Matile, *Org. Biomol. Chem.*, 2007, **5**, 3000-3012.
52 V. Gorteau, M. D. Julliard and S. Matile, *J. Membr. Sci.*, 2008, **321**, 37-42.
53 A. Perez-Velasco, V. Gorteau and S. Matile, *Angew. Chem. Int. Ed.*, 2008, **47**, 921-923.
54 R. I. Díaz, J. Regourd, P. V. Santacroce, J. T. Davis, D. L. Jakeman and A. Thompson, *Chem. Commun.*, 2007, 2701-2703.
55 P. A. Gale, J. Garric, M. E. Light, B. McNally and B. D. Smith, *Chem. Commun.*, 2007, 1736-1738.
56 P. V. Santacroce, J. T. Davis, M. E. Light, P. A. Gale, J. C. Iglesias-Sanchez, P. Prados and R. Quesada, *J. Am. Chem.Soc.*, 2007, **129**, 1886-1887.
57 J. T. Davis, P. A. Gale, O. A. Okunola, P. Prados, J. C. Iglesias-Sanchez, T. Torroba and R. Quesada, *Nat. Chem.*, 2009, **1**, 138-144.
58 X. Li, B. Shen, X.-Q. Yao and D. Yang, *J. Am. Chem. Soc.*, 2007, **129**, 7264-7263.
59 X. Li, B. Shen, X.-Q. Yao and D. Yang, *J. Am. Chem. Soc.*, 2009, **131**, 13676-13680.
60 S. K. Berezin and J. T. Davis, *J. Am. Chem. Soc.*, 2009, **131**, 2458-2459.
61 W. M. Leevy, S. T. Gammon, H. Jiang, J. R. Johnson, D. J. Maxwell, E. N. Jackson, M. Marquez, D. Piwnica-Worms and B. D. Smith, *J. Am. Chem. Soc.*, 2006, **128**, 16476-16477.
62 W. M. Leevy, J. R. Johnson, C. Lakshmi, J. Morris, M. Marquez and B. D. Smith, *Chem. Commun.*, 2006, 1595-1597.
63 B. McNally, E. J. O'Neil, A. Nguyen and B. D. Smith, *J. Am. Chem. Soc.*, 2008, **130**, 17274-17275.
64 P. R. Brotherhood and A. P. Davis, *Chem. Soc. Rev.*, 2010, **39**, 3633-3647.
65 B. A. McNally, A. V. Koulov, T. N. Lambert, B. D. Smith, J. B. Joos, A. L. Sisson, J. P. Clare, V. Sgarlata, L. W. Judd, G. Magro and A. P. Davis, *Chem. Eur. J.*, 2008, **14**, 9599-9606.
66 X. Z. Lai, Y. Feng, J. Pollard, J. N. Chin, M. J. Rybak, R. Bucki, R. F. Epand, R. M. Epand and P. B. Savage, *Acc. Chem. Res.*, 2008, **41**, 1233-1240.
67 R. F. Epand, P. B. Savage and R. M. Epand, *Biochim. Biophys. Acta*, 2007, **1768**, 2500-2509.
68 W.-H. Chen, X.-B. Shao, R. Moellering, C. Wennersten and S. L. Regen, *Bioconjugate Chem.*, 2006, **17**, 1582-1591.
69 S. D. Whitmarsh, A. P. Redmond, V. Sgarlata and A. P. Davis, *Chem. Commun.*, 2008, 3669-3671.
70 V. Janout and S. L. Regen, *Bioconjugate Chem.*, 2009, **20**, 183-192.
71 M. Kondo, M. Mehiri and S. L. Regen, *J. Am. Chem. Soc.*, 2008, **130**, 13771-13777.
72 M. Mehiri, W.-H. Chen, V. Janout and S. L. Regen, *J. Am. Chem. Soc.*, 2009, **131**, 1338-1339.
73 W.-H. Chen, V. Janout, M. Kondo, A. Mosoian, G. Mosoyan, R. R. Petrov, M. E. Klotman and S. L. Regen, *Bioconjugate Chem.*, 2009, **20**, 1711-1715.
74 R. R. Petrov, W.-H. Chen and S. L. Regen, *Bioconjugate Chem.*, 2009, **20**, 1037-1043.
75 C. C. Tong, R. Quesada, J. L. Sessler and P. A. Gale, *Chem. Commun.*, 2008, 6321-6324.
76 M. G. Fisher, P. A. Gale, J. R. Hiscock, M. B. Hursthouse, M. E. Light, F. P. Schmidtchen and C. C. Tong, *Chem. Commun.*, 2009, 3017-3019.
77 S. Licen, C. Coppola, J. D'Onofrio, D. Montesarchio and P. Tecilla, *Org. Biomol. Chem.*, 2009, **7**, 1060-1063.
78 I. Tabushi, Y. Kuroda and K. A. Yokota, *Tetrahedron Lett.*, 1982, **29**, 4601-4604.
79 N. Madhavan and M. S. Gin, *ChemBioChem*, 2007, **8**, 1834-1840.
80 P. V. Jog and M. S. Gin, *Org. Lett*., 2008, **10**, 3693-3696.
81 K. S. Iqbal and P. J. Cragg, *Dalton Trans.*, 2007, 26-32.
82 J. L. Seganish, P. V. Santacroce, K. J. Salimian, J. C. Fettinger, P. Zavalij and J. T. Davis, *Angew. Chem. Int. Ed.*, 2006, **45**, 3334-3338.
83 O. A. Okunola, J. L. Seganish, K. J. Salimian, P. Y. Zavalij and J. T. Davis, *Tetrahedron*, 2007, **63**, 10743-10750.
84 P. V. Santacroce, O. A. Okunola, P. Y. Zavalij and J. T. Davis, *Chem. Commun.*, 2006, 3246-3248.
85 W. D. Seufert, *Nature*, 1965, **207**, 174-176.
86 K. S. Iqbal, M. C. Allen, F. Fucassi and P. J. Cragg, *Chem. Commun.*, 2007, 3951-3953.
87 O. Lawal, K. S. J. Iqbal, A. Mohamadi, P. Razavi, H. T. Dodd, M. C. Allen, S. Siddiqui, F. Fucassi and P. J. Cragg, *Supramol. Chem.*, 2009, **21**, 55-60.
88 I. Izzo, S. Licen, N. Maulucci, G. Autore, S. Marzocco, P. Tecilla and F. De Riccardis, *Chem. Commun.*, 2008, 2986-2988.
89 V. Paquet, A. Zumbuehl and E. M. Carreira, *Bioconjugate Chem.*, 2006, **17**, 1460-1463.
90 M. Tsikolia, A. C. Hall, C. Suarez, Z. O. Nylander, S. M. Wardlaw, M. E. Gibson, K. L. Valentine, L. N. Onyewadume, D. A. Ahove, M. Woodbury, M. M. Mongare, C. D. Hall, Z. Wang, B. Draghici and A. R. Katritzky, *Org. Biomol. Chem.*, 2009, **7**, 3862-3870.
91 M. E. Weber, E. K. Elliott and G. W. Gokel, *Org. Biomol. Chem.*, 2006, **4**, 83-89.
92 M. E. Weber, W. Wang, S. E. Steinhardt, M. R. Gokel, W. M. Leevy and G. W. Gokel, *New J. Chem.*, 2006, **30**, 177-184.
93 W. Wang, C. R. Yamnitz and G. W. Gokel, *Heterocycles*, 2007, **73**, 825-839.
94 J. C. Iglesias-Sánchez, W. Wang, R. Ferdani, P. Prados, J. de Mendoza and G. W. Gokel, *New J. Chem.*, 2008, **32**, 878-890.
95 W. Wang, R. Li and G. W. Gokel, *Chem. Eur. J.*, 2009, **15**, 10543-10553.
96 W. Wang, R. Li and G. W. Gokel, *Chem. Commun*., 2009, 911-913.
97 A. Cazacu, C. Tong, A. van der Lee, T. M. Fyles and M. Barboiu, *J. Am. Chem. Soc.*, 2006, **128**, 9541-9548.
98 R. J. Brea, C. Reiriz and J. R. Granja, *Chem. Soc. Rev.*, 2010, **26**, 1448-1456.
99 C. De Cola, S. Licen, D. Comegna, E. Cafaro, G. Bifulco, I. Izzo, P. Tecilla and F. De Riccardis, *Org. Biomol. Chem.*, 2009, **7**, 2851-2854.
100 B. Gong, *Acc. Chem. Res.*, 2008, **41**, 1376-1386.
101 A. J. Helsel, A. L. Brown, K. Yamato, W. Feng, L. Yuan, A. J. Clements, S. V. Harding, G. Szabo, Z. Shao and B. Gong, *J. Am. Chem. Soc.*, 2008, **130**, 15784-15785.
102 L. Fischer and G. Guichard, *Org. Biomol. Chem.*, 2010, **8**, 3101-3117.
103 A. Hennig, L. Fischer, G. Guichard and S. Matile, *J. Am. Chem. Soc.*, 2009, **131**, 16889-16895.

104 M. Ouellet, F. Otis, N. Voyer and M. Auger, *Biochim. Biophys. Acta*, 2006, **1758**, 1235-1244.
105 F. Otis, N. Voyer, A. Polidori and B. Pucci, *New J. Chem*., 2006, **30**, 185-190.
106 P.-L. Boudreault and N. Voyer, *Org. Biomol. Chem.*, 2007, **5**, 1459-1465.
107 R. Ferdani and G. W. Gokel, *Org. Biomol. Chem.*, 2006, **4**, 3746-3750.
108 R. Ferdani, R. Pajewski, J. Pajewska, P. H. Schlesinger and G. W. Gokel, *Chem. Commun.*, 2006, 439-441.
109 G. A. Cook, R. Pajewski, M. Aburi, P. E. Smith, O. Prakash, J. M. Tomich and G. W. Gokel, *J. Am. Chem. Soc.*, 2006, **128**, 1633-1638.
110 L. You, R. Ferdani and G. W. Gokel, *Chem. Commun.*, 2006, 603-605.
111 R. Pajewski, R. Garcia-Medina, S. L. Brody, W. M. Leevy, P. H. Schlesinger and G. W. Gokel, *Chem. Commun.*, 2006, 329-331.
112 R. Ferdani, R. Li, R. Pajewski, J. Pajewska, R. K. Winter and G. W. Gokel, *Org. Biomol. Chem.*, 2007, **5**, 2423-2432.
113 E. K. Elliott, K. J. Stine and G. W. Gokel, *J. Membr. Sci.*, 2008, **321**, 43-50.
114 L. You, R. Li and G. W. Gokel, *Org. Biomol. Chem.*, 2008, **6**, 2914-2923.
115 L. You, R. Ferdani, R. Li, J. P. Kramer, R. E. K. Winter and G. W. Gokel, *Chem. Eur. J.*, 2008, **14**, 382-396.
116 L. You and G. W. Gokel, *Chem. Eur. J.*, 2008, **14**, 5861-5870.
117 E. K. Elliott, M. M. Daschbach and G. W. Gokel, *Chem. Eur. J.*, 2008, **14**, 5871-5879.
118 S. Das, D. Seebach and R. N. Reusch, *Biochemistry*, 2002, **41**, 5307-5312.
119 T. M. Fyles, C. W. Hu and H. Luong, *J. Org. Chem.*, 2006, **71**, 8545-8551.
120 T. M. Fyles and H. Luong, *Org. Biomol. Chem.*, 2009, **7**, 725-732.
121 T. M. Fyles and H. Luong, *Org. Biomol. Chem.*, 2009, **7**, 733-738.
122 X. Chen, H. Tang, J. Wang, M. A. Even, G. N. Tew and Z. Chen, *J. Am. Chem. Soc.*, 2006, **128**, 2711-2714.
123 Y. Ishitsuka, L. Arnt, J. Majewski, S. Frey, M. Ratajczek, K. Kjaer, G. N. Tew and K. Y. Lee, *J. Am. Chem. Soc.*, 2006, **128**, 13123-13129.
124 L. Arnt, J. Rennie, S. Linser, R. Willumeit and G. N. Tew, *J. Phys. Chem. B*, 2006, **110**, 3527-3532.
125 L. Yang, V. D. Gordon, A. Mishra, A. Som, K. R. Purdy, M. A. Davis, G. N. Tew and G. C. L. Wong, *J. Am. Chem. Soc.*, 2007, **129**, 12141-12147.
126 L. Yang, V. D. Gordon, D. R. Trinkle, N. W. Schmidt, M. A. Davis, C. DeVries, A. Som, J. E. Cronan, Jr., G. N. Tew and G. C. L. Wong, *Proc. Natl. Acad. Sci. USA*, 2008, **105**, 20595-20600.
127 A. Som and G. N. Tew, *J. Phys. Chem. B*, 2008, **112**, 3495-3502.
128 A. Som, L. Yang, G. Wong and G. N. Tew, *J. Am. Chem. Soc.*, 2009, **131**, 15102-15103.
129 M. S. Kaucher, M. Peterca, A. E. Dulcey, A. J. Kim, S. A. Vinogradov, D. A. Hammer, P. A. Heiney and V. Percec, *J. Am. Chem. Soc.*, 2007, **129**, 11698-11699.
130 A. J. Kim, M. S. Kaucher, K. P. Davis, M. Peterca, M. R. Imam, N. A. Christian, D. H. Levine, F. S. Bates, V. Percec and D. A. Hammer, *Adv. Funct. Mat*., 2009, **19**, 2930-2936.
131 D. Ronan, D. Jeannerat, A. Pinto, N. Sakai and S. Matile, *New J. Chem*., 2006, **30**, 168-176.
132 F. Mora, D.-H. Tran, N. Oudry, G. Hopfgartner, D. Jeannerat, N. Sakai and S. Matile, *Chem. Eur. J.*, 2008, **14**, 1947-1953.
133 H. Tanaka, S. Litvinchuk, G. Bollot, J. Mareda, D,-H. Tran, N. Sakai and S. Matile, *J. Am. Chem. Soc.*, 2006, **128**, 16000-16001.
134 H. Tanaka, G. Bollot, J. Mareda, S. Litvinchuk, D.-H. Tran, N. Sakai and S. Matile, *Org. Biomol. Chem.*, 2007, **5**, 1369-1380
135 S. Hagihara, L. Gremaud, G. Bollot, J. Mareda and S. Matile, *J. Am. Chem. Soc*., 2008, **130**, 4347-4351.
136 S. Litvinchuk, H. Tanaka, T. Miyatake, D. Pasini, T. Tanaka, G. Bollot, J. Mareda and S. Matile, *Nat. Mater*., 2007, **6**, 576-580.
137 S. M. Butterfield, D.-H. Tran, H. Zhang, G. D. Prestwich and S. Matile, *J. Am. Chem. Soc.*, 2008, **130**, 3270-3271.
138 H. Tanaka and S. Matile, *Chirality*, 2008, **20**, 307-312.
139 A. Hennig and S. Matile, *Chirality*, 2009, **21**, 145-151.
140 S. Hagihara, H. Tanaka and S. Matile, *J. Am. Chem. Soc.*, 2008, **130**, 5656-5657.
141 S. Hagihara, H. Tanaka and S. Matile, *Org. Biomol. Chem.*, 2008, **6**, 2259-2262.
142 C. Tribet, R. Audebert, and J.-L. Popot, *Proc. Natl. Acad. Sci. USA*, 1996, **93**, 15047-15050.
143 S.-M. Lee, H. Chen, C. M. Dettmer and T. V. O Nguyen, *J. Am. Chem. Soc.*, 2007, **129**, 15096-15097.
144 Y. Luan and L. Ramos, *J. Am. Chem. Soc*., 2007, **129**, 14619-14624.
145 Y. Fan, Y. Han and Y. Wang, *J. Phys. Chem. B*, 2007, **111**, 10123-10129.
146 F. Vial, A. G. Oukhaled, L. Auvray and C. Tribet, *Soft Matter*, 2007, **3**, 75-78.
147 H.-C. Chiu, Y.-W. Lin, Y.-F. Huang, C.-K. Chuang, C.-S. Chern, *Angew. Chem. Int. Ed.*, 2008, **47**, 1875-1878.
148 N. Badi, L. Auvray and P. Guegan, *Adv. Mater.*, 2009, **21**, 4054-4057.
149 R. F. Epand, M. A. Schmitt, S. H. Gellman and R. M. Epand, *Biochim. Biophys. Acta*, 2006, **1758**, 1343-1350.
150 R. F. Epand, B. P. Mowery, S. E. Lee, S. S. Stahl, R. I. Lehrer, S. H. Gellman and R. M. Epand, *J. Mol. Biol.*, 2008, **379**, 38-50.
151 B. P. Mowery, S. E. Lee, D. A. Kissounko, R. F. Epand, R. M. Epand, B. Weisblum, S. S. Stahl and S. H. Gellman, *J. Am. Chem. Soc.*, 2007, **129**, 15474-15476.
152 B. P. Mowery, A. H. Linder, B. Weisblum, S. S. Stahl and S. H. Gellman, *J. Am. Chem. Soc.*, 2009, **131**, 9735-9745.
153 G. N. Tew, R. W. Scott, M. L. Klein and W. F. Degrado, *Acc. Chem. Res.*, 2010, **43**, 30-39.
154 S. Choi, A. Isaacs, D. Clements, D. Liu, H. Kim, R. W. Scott, J. D. Winkler, and W. F. DeGrado, *Proc. Natl. Acad. Sci. USA*, 2009, **106**, 6968-6973.
155 E. F. Palermo, I. Sovadinova and K. Kuroda, *Biomacromolecules*, 2009, **10**, 3098-3107.
156 K. Kuroda, G. A. Caputo and W. F. DeGrado, *Chem. Eur. J.*, 2009, **15**, 1123-1133.
157 I. Ivanov, S. Vemparala, V. Pophristic, K. Kuroda, W. F. DeGrado, J. A. McCammon and M. L. Klein, *J. Am. Chem. Soc.*, 2006, **128**, 1778-1779.
158 E. F. Palermo and K. Kuroda, *Biomacromolecules*, 2009, **10**, 1416–1428.
159 K. Lienkamp and G. N. Tew, *Chem. Eur J.*, 2009, **15**, 11784-11800.
160 G. J. Gabriel, J. Pool, A. Som, J. M. Dabkowski, E. B. Coughlin, M. Muthukumar and G. N. Tew, *Langmuir*, 2008, **24**, 12489-12495.
161 A. Hennig, G. J. Gabriel, G. N. Tew and S. Matile, *J. Am. Chem. Soc.*, 2008, **130**, 10338-10344.
162 S. C. Semple, A. Akinc, J. Chen, A. P. Sandhu, B. L. Mui, C. K. Cho, D. W. Y. Sah, D. Stebbing, E. J. Crosley, E. Yaworski, I. M. Hafez, J. R. Dorkin, J. Qin, K. Lam, K. G. Rajeev, K. F. Wong, L. B. Jeffs, L. Nechev, M. L. Eisenhardt, M. Jayaraman, M. Kazem, M. A. Maier, M. Srinivasulu, M. J. Weinstein, Q. Chen, R. Alvarez, S. A. Barros, S. De, S. K. Klimuk, T. Borland., V. Kosovrasti, W. L. Cantley, Y. K. Tam, M. Manoharan, M. A. Ciufolini, M. A. Tracy, A. de Fougerolles, I. MacLachlan, P. R. Cullis, T. D. Madden and M. J. Hope, *Nat. Biotechnol.*, 2010, **28**, 170-176.
163 M. Mével, N. Kamaly, S. Carmona, M. H. Oliver, M. R. Jorgensen, C. Crowther, F. H. Salazar, P. L. Marion, M. Fujino, Y. Natori, M. Thanou, P. Arbuthnot, J.-J. Yaouanc, P. A. Jaffrès and A. D. Miller, *J. Contr. Release*, 2010, **143**, 222–232.
164 V. Ciccarone, Y. Chu, K. Schifferli, J.-P. Pichet, P. Hawley-Nelson, K. Evans, L. Roy and S. Bennett, *Focus*, 1999, **21**, 54-55.
165 T. Miyatake, M. Nishihara and S. Matile, *J. Am. Chem. Soc.*, 2006, **128**, 12420-12421.
166 S. M. Butterfield, T. Miyatake and S. Matile, *Angew. Chem. Int. Ed.*, 2009, **48**, 325-328.
167 T. Takeuchi, N. Sakai and S. Matile, *Faraday Discuss*., 2009, **143**, 187-203.
168 T. Takeuchi, V. Bagnacani, F. Sansone and S. Matile, *ChemBioChem*, 2009, **10**, 2793-2799.
169 T. Takeuchi and S. Matile, *J. Am. Chem. Soc.*, 2009, **131**, 18048-18049.

Biodata

Stefan Matile received his education from Professor Wolf Woggon at the University of Zurich (Diploma 1989, PhD 1994) and Professor Koji Nakanishi at Columbia University, New York (postdoc, 1994-1996). After three years as Assistant Professor at Georgetown University, Washington DC (1996-1999), he moved to the University of Geneva (1999), where he is currently Full Professor and ERC Advanced Investigator in the Department of Organic Chemistry and the NCCR Chemical Biology. His research interests include functional biosupramolecular systems for broad applications such as organic solar cells or biosensors.

Andreas Vargas Jentzsch received his education from the University of Geneva. His undergraduate studies have been supported by a fellowship from the Fondation Simon I. Patiño. In 2009, he started a PhD under the supervision of Professor Stefan Matile. His current research focuses on the use of unusual interactions in synthetic transport systems, including anion-π interactions.

Javier Montenegro received his MS (2004) and his PhD (2009) from Professor Susana Lopez at the University of Santiago de Compostela, Spain, working on the synthesis and evaluation of artificial retinoids. In 2009, he moved to the University of Geneva, Switzerland, for a postdoc under the supervision of Professor Stefan Matile. His research is focused on the design and synthesis of membrane-based differential sensing systems and dynamic polyion-counterion delivery systems for interference RNA.

Andrea Fin received his MS in 2008 from the University of Turin, Italy. Since November 2008, he is a PhD student at the University of Geneva, Switzerland, under the supervision of Professor Stefan Matile. His research is focused on the design and synthesis of dynamic fluorescent probes to visualize lipid bilayer membranes and illuminate processes such cellular uptake.